

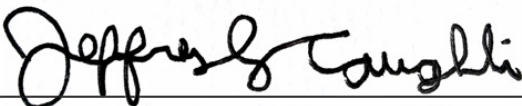


# ***Kepler: A Search for Terrestrial Planets***

Description of the TCERT Vetting  
Reports for Data Release 25

KSCI-19105-002  
Jeffrey L. Coughlin  
September 21, 2017

NASA Ames Research Center  
Moffet Field, CA 94035

Prepared by:  Date: 9/21/17  
Jeffrey L. Coughlin, *Kepler* Science Office

Approved by:  Date: 9/21/17  
Natalie Batalha, *Kepler* Project Scientist

Approved by:  Date: 9/21/17  
Michael R. Haas, *Kepler* Science Office Director

## Table of Contents

PREFACE.....	4
KIC/TCE Cover Page.....	5
Page 1 – DV Summary.....	5
Detrended Lightcurve.....	5
Phase-curve.....	8
Odd-even Test.....	10
Weak Secondary Test.....	10
Out of Transit Centroid Offsets.....	12
DV Analysis Table.....	14
Pages 2 & 3 – PDC Flux Plots.....	18
Page 4 & 5 – Odd/Even Plots.....	20
Page 6 – Non-Whitened vs. Whitened Light Curves.....	21
Pages 7, 8, & 9 – Multi-Quarter Transit Plots.....	22
Pages 10 and 11 – Modelshift Uniqueness Test and Occultation Search.....	23
Modelshift Uniqueness and Occultation Test Theory.....	27
Modelshift Metrics.....	28
Phased Lightcurve.....	31
Model Filtered Data.....	31
Primary, Secondary, Tertiary, Positive, Odd, and Even Events.....	31
Page 12 – Stellar Parameters and Secondary Eclipse Tables.....	33
Page 13 – Centroid Analysis Overview.....	35
Pages 14-18 – Pixel-Level Images.....	36
Page 18 – Folded Flux and Flux-Weighted Centroid Time Series.....	37
Page 19 – UKIRT Image.....	37
Page 20 and Beyond.....	38
References.....	41

## PREFACE

The Q1–Q17 DR25 TCERT Vetting Reports are a collection of plots and diagnostics used by the Threshold Crossing Event Review Team (TCERT) to evaluate threshold crossing events (TCEs). While designation of Kepler Objects of Interest (KOIs) and classification of them as Planet Candidates (PCs) or False Positives (FPs) is completely automated via a robotic vetting procedure (the Robovetter) for the Q1–Q17 DR25 planet catalog, as described in Thompson et al. (2017), these reports help to visualize the metrics used by the Robovetter and evaluate those robotic decisions for individual objects. For each Q1–Q17 DR25 TCE, these reports include the following products: (a) the DV one-page summary, (b) selected pertinent diagnostics and plots from the full DV report, and (c) additional plots and diagnostics not included in the full DV report, including an alternate means of data detrending.

As part of the DR25 catalog creation process, the *Kepler* pipeline was run on the observed (OBS) data, the data containing artificially injected transits (INJ), the data that is flux inverted (INV), and the data that is temporally scrambled (SCR). The TCEs detected in the OBS data are referred to as obsTCEs. The INJ data (see Christiansen, 2017) was divided into three groups: 1) injections of single transiting planets at the nominal positions of their target stars, 2) injections of single planets positionally off-target (i.e., they were injected with a centroid offset), and 3) injections of two on-target planets on each star with the same period, but different epochs, to simulate a population of eclipsing binaries (EBs). The injections that were successfully detected as TCEs are referred to as the inj1TCEs, inj2TCEs, and inj3TCEs for the three groups, respectively. For the INV data, the pipeline was re-run with the light curves inverted immediately before the planet search to produce inverted TCEs (invTCEs). For the SCR data, the light curves were scrambled by re-arranging the data in per-quarter or per-year chunks immediately before the planet search to produce scrambled TCEs (scrTCEs). Note that three different scrambling orders were run to create scr1TCEs, scr2TCEs, and scr3TCEs — for details on how each run was scrambled, see Coughlin (2017).

This document describes the plots and metrics presented on each page of a TCERT Vetting Report and how they can be used to determine if a TCE is a PC or FP. Vetting Reports exist for every Q1–Q17 DR25 TCE vetted by Thompson et al. (2017), including TCEs from the OBS, INJ, INV, and SCR data groups. Note this means the Vetting Reports do not include “rogue” TCEs, which were discovered after the obsTCE table was created and Twicken et al. (2016) was published. Rogue TCEs are signals that should have failed the “three-transit weight check” (see Section 2 of Burke & Catanzarite, 2017) in the transit planet search (TPS) module, but were inadvertently made into TCEs due to an error in the code. There were 1,498 rogue TCEs among the original set of 34,032 obsTCEs. Because these rogue TCEs are not modeled by the occurrence rate products which characterize the TPS module, they should not be included in occurrence rate calculations. Consequently, only the remaining set of 32,534 obsTCEs were vetted by the Robovetter to produce the KOIs found in the DR25 KOI catalog (Thompson et al., 2017).

Any questions about these reports, or the content therein, can be directed to the Kepler helpdesk (E-mail: [keplergo@mail.arc.nasa.gov](mailto:keplergo@mail.arc.nasa.gov); Website: <https://keplerscience.arc.nasa.gov/helpdesk.html>) or the Kepler Science Office (E-mail: [kepler-scienceoffice@lists.nasa.gov](mailto:kepler-scienceoffice@lists.nasa.gov)).

When citing this document, please use the following reference: Coughlin, J. L. 2017, Description of the TCERT Vetting Reports for Data Release 25 (KSCI-19105-002)

## ***KIC/TCE Cover Page***

All TCEs originating from the same KIC target are grouped into a single PDF. The first page is a cover page that shows the KIC ID listed at the top, and contains a table that lists every TCE belonging to the given KIC with each TCE's period, epoch, depth, duration, MES, SNR of the transit fit, stellar radius, stellar temperature, inferred planetary radius, and inferred planetary insolation flux. The dataset (OBS, INJ1, INJ2, INJ3, INV, SCR1, SCR2, or SCR3) is also given, and for the OBS data, the table indicates whether or not the TCE is designated as a KOI. No TCEs from simulated data (INJ, INV, SCR) are ever promoted to KOI status. A second table lists the results from the nominal DR25 Robovetter, including the run type, the disposition (PC or FP), the Robovetter disposition score, the four major disposition flags (N, S, C, and E), and a comment string containing all of the Robovetter minor flags (see Thompson et al. 2017). If the TCE was detected as a false positive due to an ephemeris match (see Coughlin et al. 2014), a third table containing information about the match is shown at the bottom of the cover page.

Throughout this document, we will show examples from the Kepler-69 system (KIC 008692861), a well-known system with two confirmed planets. We focus on Kepler-69b (Q1–Q17 DR25 TCE 008692861-01) as it is the first TCE of the system and has a high signal-to-noise ratio (SNR). The cover page for KIC 008692861 is shown in Figure 1.

## ***Page 1 – DV Summary***

The Kepler Q1–Q17 DR25 TCERT Vetting Reports have 19 additional pages for each TCE. Page 1 (Figure 2) contains the Data-Validation (DV) one-page summary that highlights some of the tests and figures from the associated full DV report. DV reports are always available and people are encouraged to make use of them when the summaries prove insufficient.

Each panel in Figure 2 is discussed separately below, but briefly, the top panel shows the photometric time-series, and underneath is the photometric time-series folded on the period of the candidate event. To the right is the best candidate for a secondary eclipse in the data. Below and to the left is the phase-curve zoomed in on the transit event. To the right is the phase-curve zoomed in on the transit event, but binned and shown in the whitened domain. In addition, this plot shows the residuals from the best-fit model and the whitened light curve at a phase of 0.5. The bottom row has the odd-even transit plot on the left, a centroid snapshot in the center, and a table of model parameters to the right.

## ***Detrended Lightcurve***

The top panel of the DV summary is repeated in Figure 3. This figure shows the detrended *Kepler* long-cadence photometric time-series. Above this plot the user can find the Kepler identifier (in this example 008692861), the candidate number (1 of 2) and the measured orbital period (13.722 d). If the DV module federated the period and epoch of the TCE to an existing KOI at the time of generation, the next line will contain the KOI number, Kepler confirmed planet number if it exists, and ephemeris correlation (Corr.) metric. On the last line is the Kepler magnitude (Kp:13.75), the estimated stellar radius in solar units ( $R_*$ : 0.94  $R_s$ ), the stellar effective temperature (Teff: 5637.0 K), the stellar surface gravity in cgs units (logg: 4.40) and the metallicity scaled to solar ([Fe/H]: -0.300). The plot itself

shows relative flux versus time. The red, dashed vertical lines mark the beginning of each quarter of observations. The quarter and CCD channel number are marked next to each line along the top of the panel. In the example shown, the target was located on channel [8.1] in Q3, on channel [12.1] in Q4, etc. Along the bottom axis there are triangle markers that indicate the location of each transit. For very short orbital periods, the markers along the bottom overlap and appear as a thick line.

Only the deepest transit events will be apparent in this figure; most moderate to low SNR events only become apparent in the phased and binned data plots. However, users should be alert for significant outliers that align with the marked transits or changes in the noise properties with a periodicity similar to the transit period.

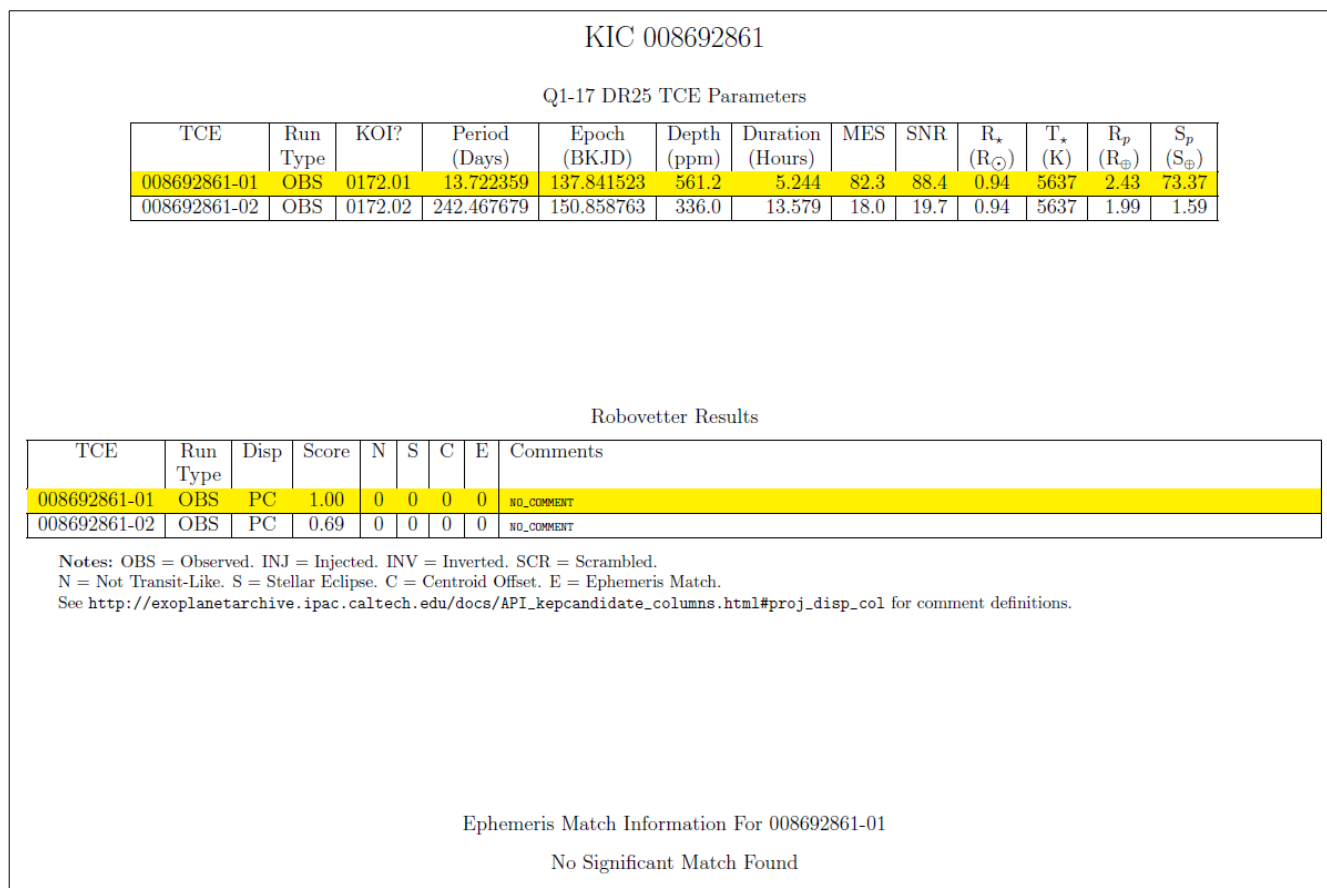


Figure 1: The cover page tabulates all TCEs found on the KIC ID shown at the top. The first table lists each TCE along with the run type (OBS, INV, SCR1, SCR2, SCR3, INJ1, INJ2, or INJ3), whether or not it is a KOI, as well as its period, epoch, depth, duration, MES, SNR of the transit fit, stellar radius, stellar temperature, inferred planet radius, and inferred planetary insolation flux from the DV module of the *Kepler* pipeline. The second table lists each TCE, the run type, the disposition given by the DR25 Robovetter (PC or FP), the disposition score, the values (0 or 1) for the four major disposition flags (N, S, C, and E), and a comment string that contains the Robovetter minor disposition flags. If the highlighted TCE was declared a false positive due to an ephemeris match, a third table is shown with information on the match. For Kepler-69b (KOI 172.01), no significant ephemeris match was found.

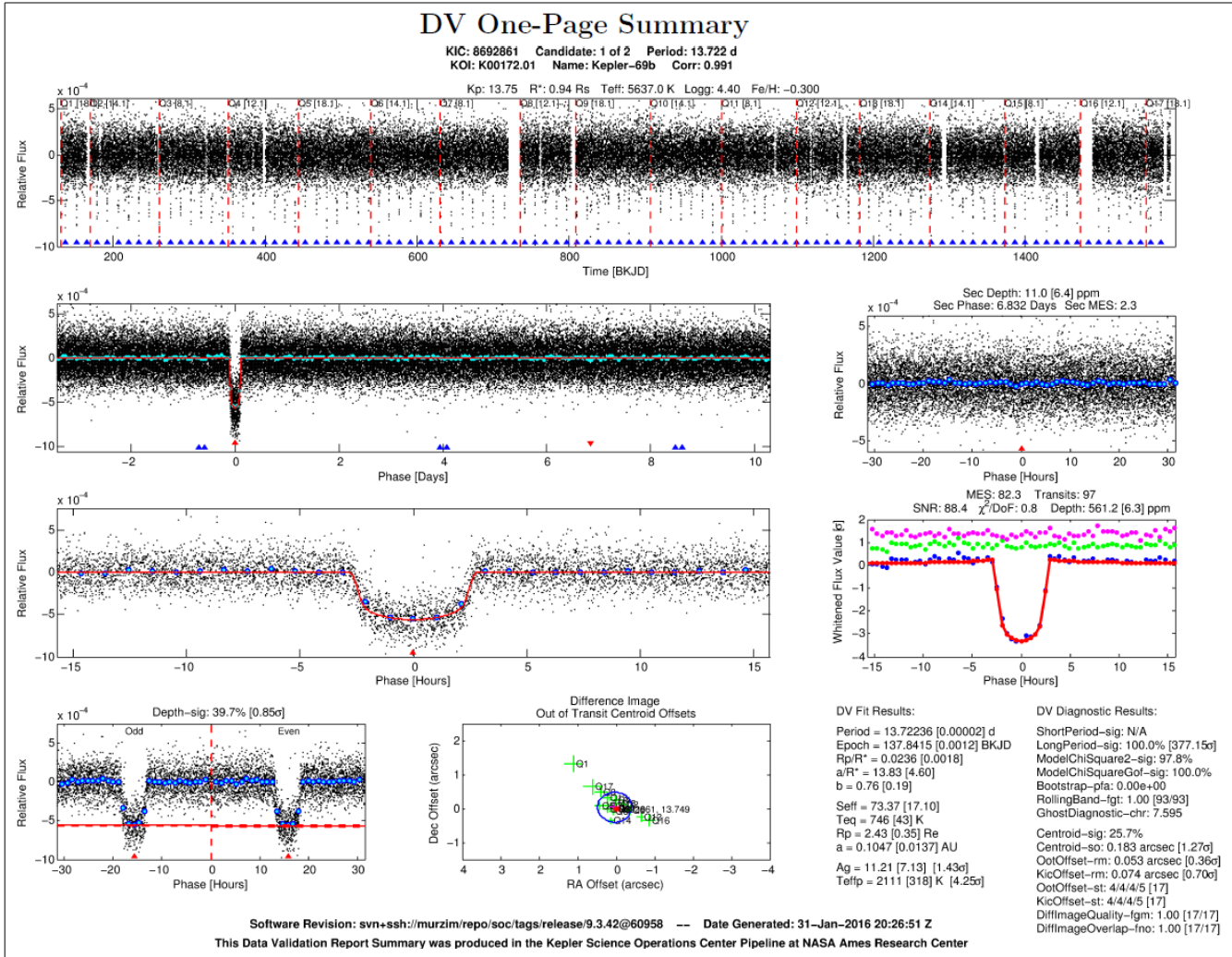


Figure 2: Page 1 of the Kepler Q1–Q17 DR25 TCERT Vetting Reports showing the DV Summary page. The example shown here is Kepler-69b (Q1–Q17 DR25 TCE 008692861-01).

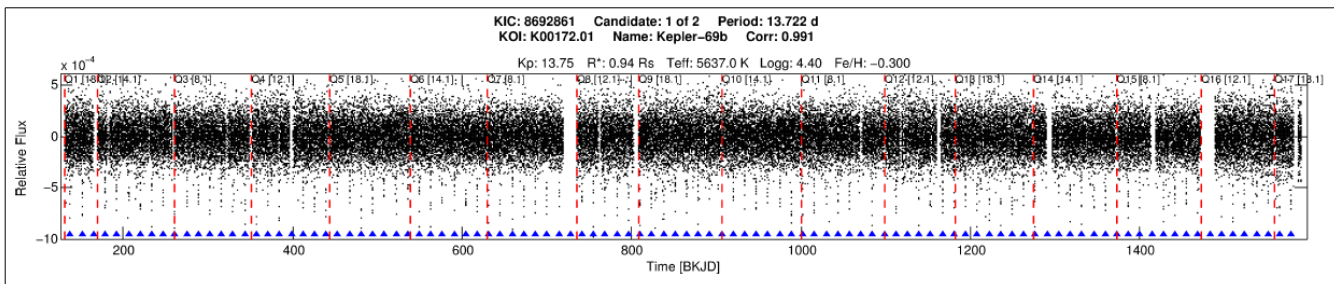


Figure 3: The detrended *Kepler* long-cadence photometric time-series. The red, dashed vertical lines mark the beginning of each quarter of photometric observations. The upward-facing, filled, black triangles along the bottom mark the location of the individual transits. The numbers in brackets next to each quarter designate the CCD channel and module that the star fell on each quarter.

### Phase-curve

Below the plot of the photometric time series, one finds the photometric phase-curve as shown in Figure 4, where the observations have been folded at the orbital period of the candidate transit event. The best-fit model is shown as a red line, and binned points are shown via blue-circled, cyan-filled points. Along the bottom, the upward-facing, red triangle denotes the location of the primary transit event, and the downward-facing, red triangle denotes the location of the strongest secondary event detected. Upward-facing triangles of other colors denote the location of transits of other TCEs in the phase space of the current TCE under examination.

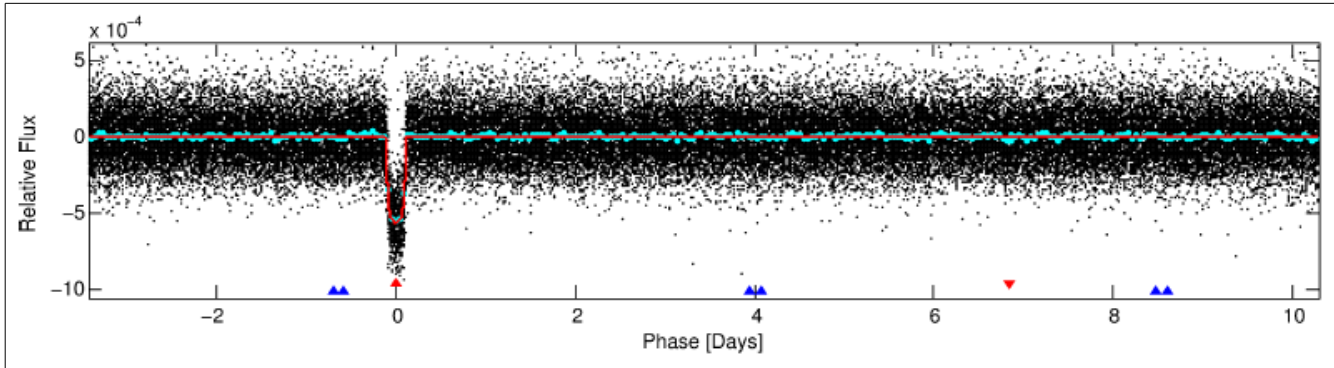


Figure 4: The photometric data folded at the orbital period of the candidate transit event. The red line shows the best-fit transit model. The blue-circled, cyan-filled points show the data binned. The transit event is located at phase 0.0 and marked with an upward-facing, red triangle. The downward-facing, red triangle marks the location of the strongest secondary event via the weak secondary test. Upward-facing triangles of other colors show the locations of the primary events of other TCEs in the system, in the phase space of the current TCE under examination.

This figure is useful for identification of the transit and possible secondary events, which may or may not generate their own TCEs. One should also examine the transit photometry and ask whether the event is consistent with a planetary transit or appears to be due to stellar variability.

In the third row on the left, there is an additional plot of the phase-folded photometry, but this time zoomed in on the transit event as shown in Figure 5. This figure is useful for judging the SNR of the transit event and its shape. While the *Kepler* pipeline fitter and DV module work with photometry in the whitened domain, this plot is shown in the flux domain, detrended using a moving median filter. Due to the window size of the median filter not being significantly longer than the transit duration, do not over-interpret any increases in the flux before ingress or after egress as signs of a photometric false-positive. We recommend using Figure 6 (discussed below), which presents the data and fit in the whitened domain, for FP identification. Figure 5 is useful for identification of the transit event, validation of the reported SNR, and noting anomalies.

At the top of Figure 6 values are listed for the MES, number of transits used in computing the MES, the SNR of the DV model fit, the reduced chi-squared value of the fit, and measured depth in ppm, with uncertainty shown in brackets. Figure 6 shows the whitened, binned, and phased photometric time-series zoomed in on the transit event, along with the whitened transit model fit, and is often one of the

most useful figures for evaluating the data and the transit model fit. If you examine Figure 6, you may see increases in the flux before ingress and after egress as the transit photometry and the model are distorted by the whitener.

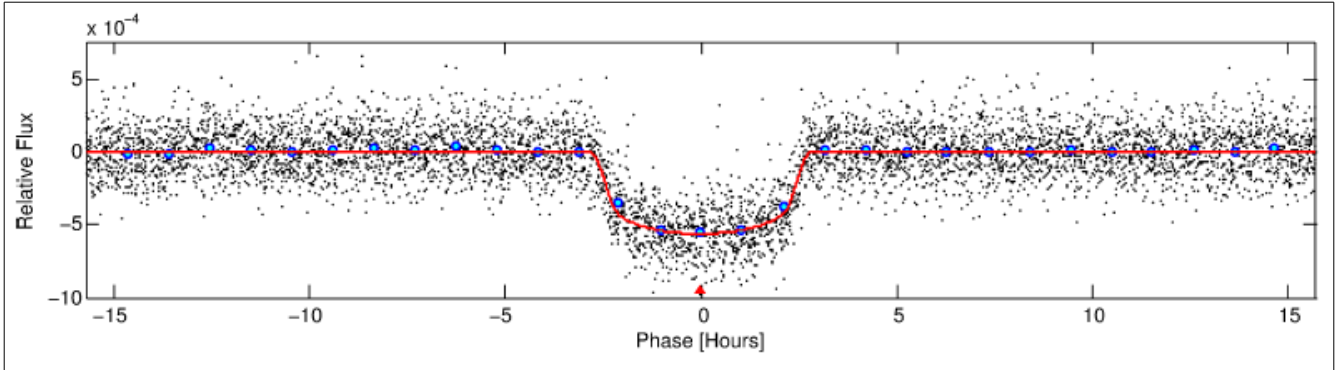


Figure 5: The phase-folded photometric time-series zoomed in on the transit event. The blue-circled, cyan-filled points show the data binned and the red line shows the best fit transit model.

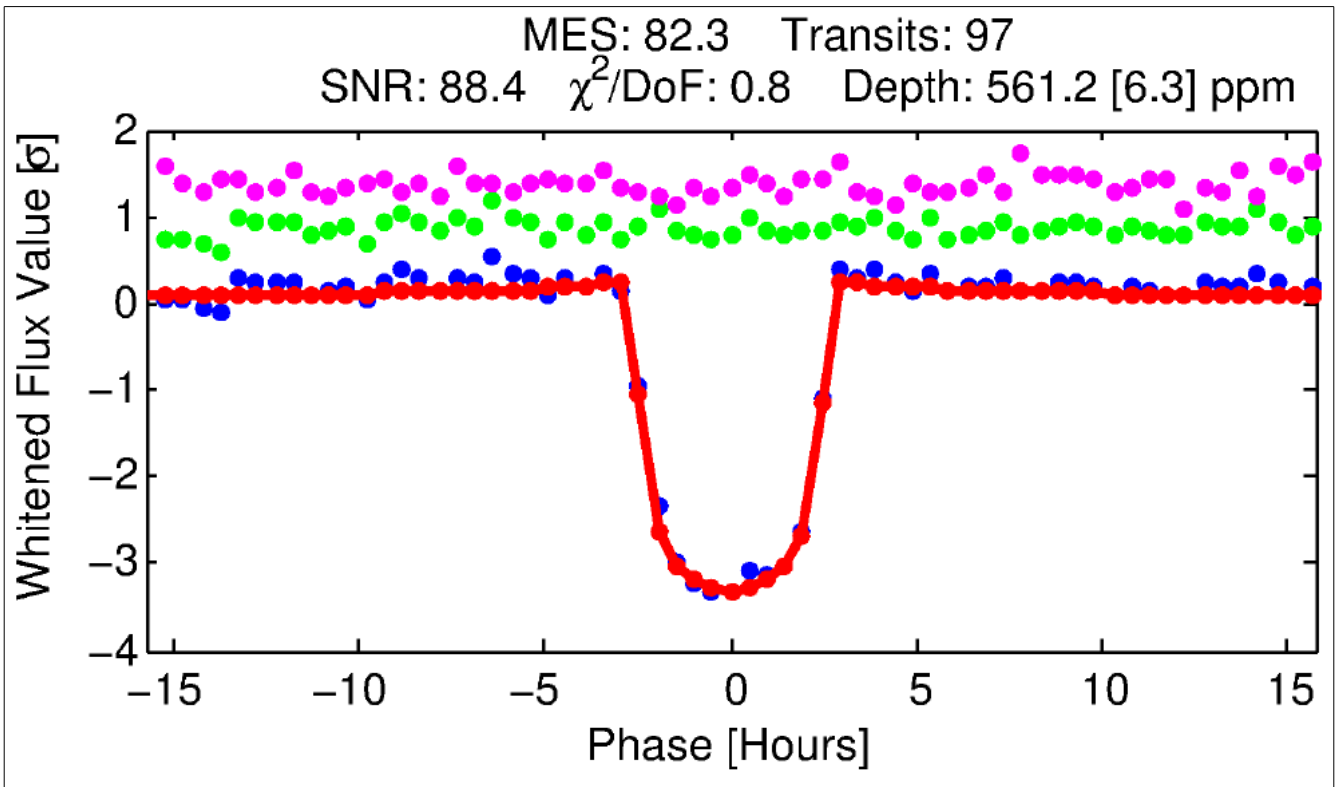


Figure 6: The whitened, binned, and phase-folded photometric time-series zoomed in on the transit event is shown by the blue points. The red line with points shows the best-fit, whitened transit model. The green points show the residuals after subtracting the best fit transit model. The magenta markers show the phased data at half the orbital phase where a potential occultation may occur for a circular orbit. The values for the MES, number of transits, the SNR of the DV model fit, the reduced chi-squared, and measured depth in ppm, with uncertainty in brackets, are listed at the top of the plot.

The user should also be aware that the transit model is restricted to have an impact parameter less than 1.0. Thus, 'V'-shaped transits due to stellar binaries and grazing transits may be poorly fit, especially when the impact parameter,  $b$ , approaches 1.0. If the model is a poor representation of the whitened transit photometry, then caution should be exercised when interpreting statistics that rely on the model fit such as the signal-to-noise, transit depth, and odd-even transit comparison.

### *Odd-even Test*

*Kepler* photometry can provide a precise measurement of the transit depth, reaching the part-per-million (ppm) level with multiple transits. Determination and comparison of the transit depths for odd-numbered transits (the first, third, fifth, etc) with the transit depths for even-numbered transits (the second, fourth, sixth, etc) can provide a powerful test of whether a transit event is consistent with an extrasolar planet interpretation or not. A common false-positive is an eclipsing binary system composed of two stars with nearly equal mass, size, and temperature. This type of false-positive may be detected by TPS at half the true period of the system, showing alternating eclipses with slightly different depths.

Figure 7 presents the *Kepler* photometry for the odd-numbered transits on the left panel butted up against the even-numbered transits in the right panel. The difference in the odd- and even-numbered transits is determined by the DV transit model fit to each set independently, and is used to estimate the probability that the depths are different. The calculation is presented above the odd-even plot as shown in Figure 7. The Depth-sig metric determines if the depths are similar (100%) or different (0%) and is alternately reported as a sigma confidence level of their difference. This calculation depends on the transit model being a good representation of the transit photometry (see Figures 4–6) and assumes that there are no systematics present in the photometry, such as data outliers.

The odd-even test will fail when astrophysical phenomena, such as star-spots, are present on the host star. These become an important concern when only a few transits are present. Stellar activity may produce systematic differences in the transit depths that are not properly reflected in the calculation of significance for the depth difference. Also, due to natural seasonal depth variations associated with *Kepler*'s quarterly roll, which moves targets to different detectors, the odd-even test is not effective at periods greater than  $\sim 90$  days when there is only one or fewer transits per quarter.

### *Weak Secondary Test*

Figure 8 presents the results of the Weak Secondary Test. For this test, the primary transit signal is first removed, and the whitening filter is re-applied to the light curve. The Transiting Planet Search (TPS) algorithm is then run on the resulting data with the same search duration as the primary TCE. Finally, the resulting single event detection time-series is folded at the same period as the primary TCE. This produces, among many other useful quantities, the value and phase of the Multiple Event Statistic (MES) for the strongest transit-like signal at the TCE's period, aside from the primary TCE itself.

The phased data is centered on the secondary eclipse candidate in Figure 8, with black dots representing the raw data and blue-circled, cyan-filled points representing phase-binned averages of the data. At the top of Figure 8, the depth of the secondary in ppm is given, along with the measurement

error in brackets. Below this, the values of the MES and phase of the secondary eclipse candidate (in days relative to the TCE) are displayed. If the MES is greater than 7.1 (the formal mission detection threshold) then it is colored red to indicate the secondary eclipse candidate is statistically significant.

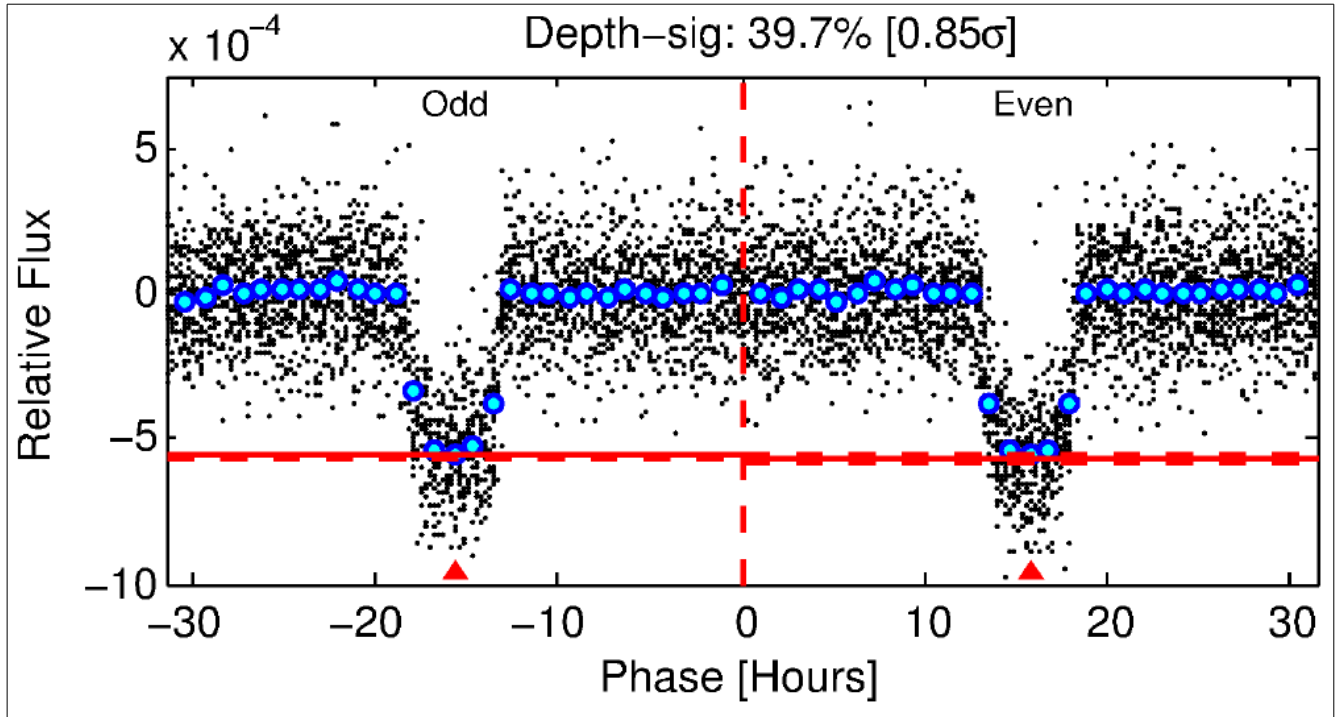


Figure 7: The odd-numbered transits are folded on top of one another and plotted in the left panel, and even-numbered transits are similarly displayed in the right panel. The vertical dashed line separates the panels. The horizontal solid lines represent the depth of the odd- and even-numbered transits separately. The two horizontal dashed lines indicate the  $\pm 1\sigma$  error limits. (In this example, the errors are small in comparison to the resolution of the plot.) The blue-circled, cyan-filled points show the data binned in phase. The upward pointing triangles mark the location of the center of the transit as measured by the model. For this TCE there is no significant difference between the odd- and even-numbered transits.

This plot helps assess whether there is a statistically significant secondary event in the phased light curve, which may indicate the candidate is an eclipsing binary, and thus not a viable planet candidate. The only exception is if the secondary eclipse could be due to planetary emission, but typically this is only observed for hot Jupiters with very short periods and results in very small secondary eclipse depths. This plot and the characteristics of the secondary eclipse candidate may also help to highlight transit-like artifacts in the data, which may cast doubt on the uniqueness of the primary TCE and thus the validity of the candidate. Vettors should be careful in the interpretation of this signal, as often there remains significant systematics in the Kepler DV data, and this test occasionally triggers on the edge of the primary TCE. To watch for this, compare the phase of the secondary (in days) with the period of the primary.

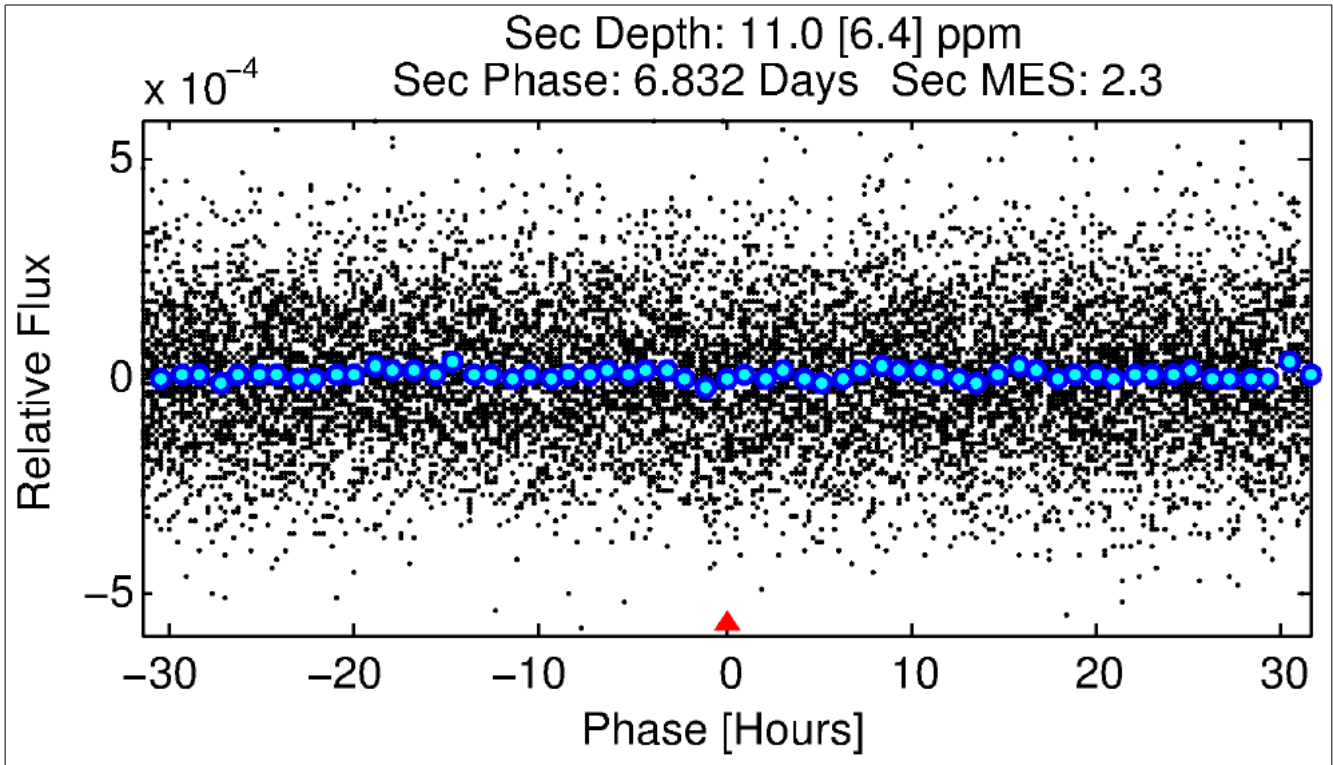


Figure 8: The strongest secondary eclipse candidate found by the weak secondary test, with the resulting phase and MES displayed above. The blue-circled, cyan-filled points represent phase-binned averages of the data. In the case of this TCE there is no significant secondary eclipse detected.

### *Out of Transit Centroid Offsets*

Figure 9 shows the PRF centroid offset with the RA Offset in arcseconds on the x-axis, and the Dec Offset in arcseconds on the y-axis. For each quarter, two separate pixel-level images of the source are computed, one using the average of only the in-transit data, and the other using the average of data just outside of transit. The difference of the in- and out-of-transit images is used to produce a difference image, which produces a star-like image at the location of the transit signal.

The Kepler Pixel Response Function (PRF) is the Kepler point spread function combined with expected spacecraft pointing jitter and other systematic effects (Bryson et al. 2010). The PRF is fit separately to the difference and out-of-transit images to compute centroid positions. The fit to the difference image gives the location of the transit source, and the fit to the out-of-transit image gives the location of the target star (assuming there are no other bright stars in the aperture). Subtracting the target star location from the transit source location gives the offset of the transit source from the target star. This calculation is performed on a per-quarter basis, and the quarterly offsets are shown as green cross-hairs and labeled with the quarter number, where the length of the arms of each cross-hair represents the  $1\sigma$  error in RA and Dec. Blue asterisks in the image show the location of known stars nearby in the aperture, with the red asterisk being the target star. (Note that in this example there are no nearby stars within the spatial extent of the plot, so no blue asterisks are shown.) The coordinate system of the plot

is chosen so that the target star is at (0,0). A robust fit (i.e., an error-weighted fit that iteratively removes extreme outliers) is performed using all the quarterly centroid offsets to compute an average in-transit offset position, and is shown with  $1\sigma$  error bars as a magenta cross. A dark blue circle is shown, always centered on the magenta cross, that represents the  $3\sigma$  limit on the magnitude of the robust-fit, quarter-averaged offset of the transit source from the target star. The numerical value of the quarterly-averaged offset source from the target star is given by `OotOffset-rm` in the DV analysis table (see Figure 10).

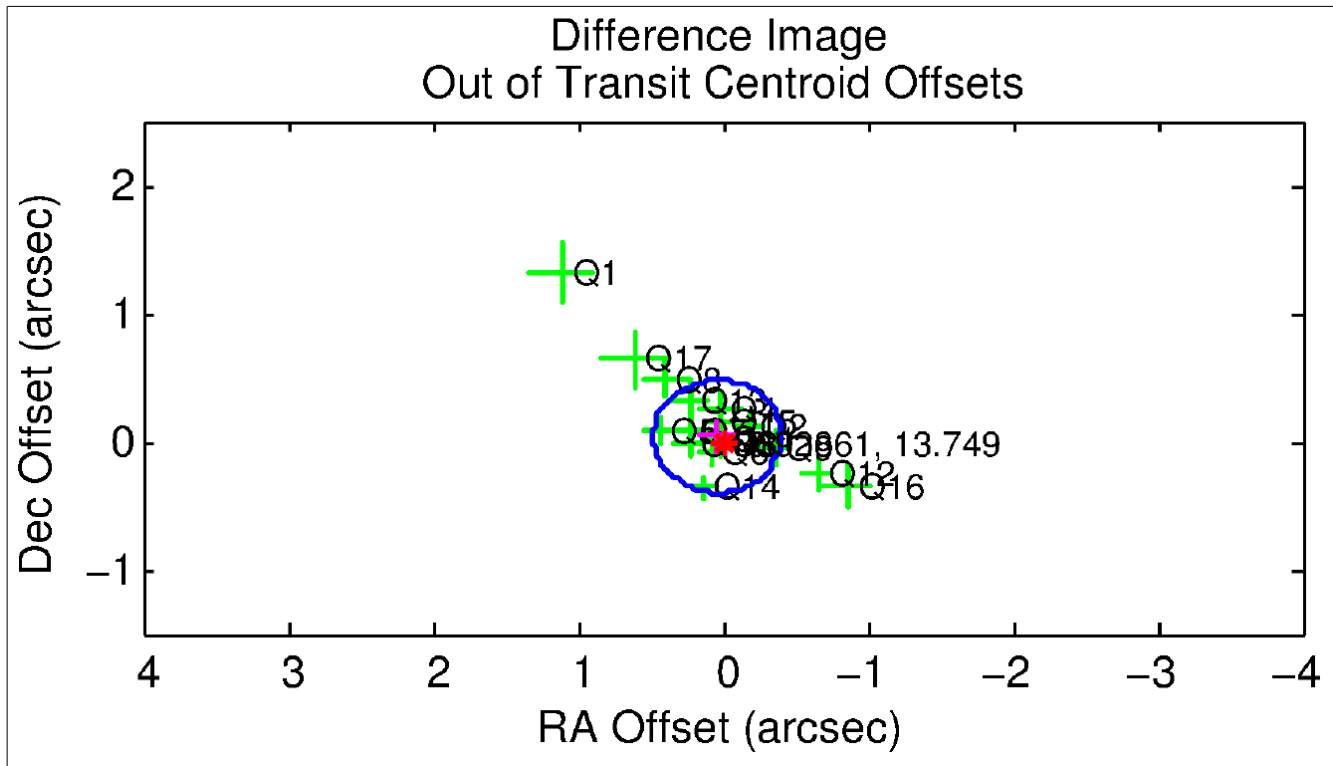


Figure 9: The PRF centroid offset plot. Individual quarterly offsets are represented by green crosses, with the size of the cross corresponding to the size of the  $1\sigma$  measurement error for that quarter. The locations of nearby stars are represented by asterisks, which are also labeled with their KIC number and Kepler magnitude. The red asterisk represents the target. The blue circle represents the  $3\sigma$  threshold for a significant centroid offset. For this TCE, nearly all of the quarterly centroid measurements lie within the blue circle (Q1 is likely an anomalous outlier) and thus there is no significant offset detected.

The plot in Figure 9 graphically indicates whether there is a significant centroid offset between the transit source and target star location during transits, and if an alternate star is likely to be the true source of the TCE. In general, a significant (i.e.,  $>3\sigma$ ) centroid offset is seen if the red asterisk lies outside the dark blue circle. In this case it is likely that the observed transit is not due to a transit on the target star. However, significant systematic noise exists in the computed centroid offsets, just as it exists in the photometric data. Thus, it is not recommended to trust any offsets to a precision of less than  $\sim 0.1''$ . As well, bright stars near the target may cause an inaccurate PRF fit, rendering the centroid results invalid. This can be checked by ensuring that the KIC position is coincident with the out-of-

transit PRF fit by comparing  $OotOffset-rm$  with the measured offset using the KIC location,  $KicOffset-rm$ , given in the DV results table, and discussed more in the next section (see Figure 10). Finally, these diagnostics are valid only if the TCE is due to a transit or eclipse on a star in the aperture. If the TCE results from a systematic error, such as a spacecraft pointing tweak, pixel sensitivity dropout, or other similar effect, then this method of measuring centroids is invalid.

### *DV Analysis Table*

Figure 10 shows a table of fit parameters, derived parameters, and vetting statistics generated by the DV analysis. The left column contains best-fit parameters from a Mandel-Agol (2002) transit model that has been fitted to the whitened data, assuming the TCE is a transiting planet. The right column contains various diagnostic parameters, most of which are used to determine the location of the transit signal relative to the target star using a variety of methods, as well as the quality of the measurements.

The parameters for the left column are:

- Period: The orbital period of the planetary candidate in days. The measurement error is shown in brackets.
- Epoch: The epoch (i.e., the central time of the first transit) shown in Barycentric Kepler Julian Date (BKJD), where  $BKJD = BJD - 2454833.0$ . The measurement error is shown in brackets.
- $R_p/R_*$ : The ratio of the planetary radius to the stellar radius. The measurement error is shown in brackets.
- $a/R_*$ : The ratio of the planet-star separation at time of transit to the stellar radius. The measurement error is shown in brackets.
- b: The impact parameter. A value of  $b = 0$  represents a central transit and  $b = 1$  represents a grazing transit where the center of the planet aligns with the limb of the star at the time of central transit. The measurement error is shown in brackets. Note that the DV fit does not allow for models with  $b > 1.0$ .
- $Seff$ : The calculated insolation flux received by the planet, in units of Earth's insolation flux. The measurement error is shown in brackets.
- $Teq$ : The calculated equilibrium temperature of the planet's surface in Kelvin. The measurement error is shown in brackets.
- $R_p$ : The calculated planetary radius in units of Earth radii. The measurement error is shown in brackets.
- a: The calculated semi-major axis of the system in AU. The measurement error is shown in brackets.
- $Ag$ : The calculated geometric albedo of the planet, given the fractional depth (D) from the weak secondary test, planetary radius ( $R_p$ ), and semi-major axis (a), such that  $Ag = D \cdot a^2 / R_p^2$ . The measurement error is shown in brackets.

DV Fit Results:	DV Diagnostic Results:
Period = 13.72236 [0.00002] d	ShortPeriod-sig: N/A
Epoch = 137.8415 [0.0012] BKJD	LongPeriod-sig: 100.0% [377.15 $\sigma$ ]
Rp/R* = 0.0236 [0.0018]	ModelChiSquare2-sig: 97.8%
a/R* = 13.83 [4.60]	ModelChiSquareGof-sig: 100.0%
b = 0.76 [0.19]	Bootstrap-pfa: 0.00e+00
Seff = 73.37 [17.10]	RollingBand-fgt: 1.00 [93/93]
Teq = 746 [43] K	GhostDiagnostic-chr: 7.595
Rp = 2.43 [0.35] Re	Centroid-sig: 25.7%
a = 0.1047 [0.0137] AU	Centroid-so: 0.183 arcsec [1.27 $\sigma$ ]
Ag = 11.21 [7.13] [1.43 $\sigma$ ]	OotOffset-rm: 0.053 arcsec [0.36 $\sigma$ ]
Teffp = 2111 [318] K [4.25 $\sigma$ ]	KicOffset-rm: 0.074 arcsec [0.70 $\sigma$ ]
	OotOffset-st: 4/4/4/5 [17]
	KicOffset-st: 4/4/4/5 [17]
	DiffImageQuality-fgm: 1.00 [17/17]
	DiffImageOverlap-fno: 1.00 [17/17]

Figure 10: The DV Analysis Table. The left column contains best-fit parameters from a Mandel-Agol (2002) transit model fitted to the whitened data, assuming the TCE is a transiting planet. The right column contains various diagnostic parameters, most of which are used to determine the location of the transit signal relative to the target star using a variety of methods, as well as the quality of the centroid measurements.

- Teffp**: The calculated planet effective temperature in Kelvin, assuming bolometric flux, based on the depth of the most significant secondary event at the period and trial pulse duration of the TCE (D), stellar effective temperature (Teff), planetary radius (Rp), and stellar radius (R\*), such that  $T_{\text{effp}} = D^{1/4} \cdot T_{\text{eff}} / (R_p/R^*)^{1/2}$ . The measurement error is shown in the first set of brackets. The difference in standard deviations between the planet effective temperature and equilibrium temperature is shown in the second set of brackets. The planet effective temperature is displayed in red if the secondary multiple event statistic exceeds the transiting planet detection threshold and the planet effective temperature is significantly greater than the equilibrium temperature.

The parameters for the right column are:

- ShortPeriod-sig**: A comparison of the period of the current TCE to the next shortest period TCE in the system. A value of 0% [0.0 $\sigma$ ] indicates a perfect match (no difference) between the two periods. Larger percentages (larger sigmas) indicate an increasing difference between the TCE periods. The text will appear in red if the two periods are considered to be significantly related. A significant value of ShortPeriod-sig may indicate that the system contains an eclipsing binary whose primary and secondary eclipse events have been detected as two different TCEs,

thus having very similar periods but different epochs. If ShortPeriod-sig has a value of "NA" it means that there is no TCE detected in the system with a shorter period than the current TCE.

- LongPeriod-sig: A comparison of the period of the current TCE to the next longest period TCE in the system. A value of 100% indicates no match at all between the two periods, with lower percentages (and lower sigmas) indicating increasingly more significant (sig) agreements between the TCE periods. A significant (small percentage, small  $\sigma$ ) value of LongPeriod-sig may indicate that the system contains an eclipsing binary whose primary and secondary eclipse events have been detected as two different TCEs, thus having very similar periods but different epochs. If LongPeriod-sig has a value of "N/A" it means that there are no TCEs detected in the system with longer periods than the current TCE.

- ModelChiSquare2-sig: The significance of the  $\chi^2_{(2)}$  discriminator as described in Twicken et al. (2016). If this value is close to 100%, then it indicates the shape of the transit events are well described by a transit model. If this value is close to 0%, then the transit events are not well described by a transit model, and the event is likely a false positive. Note that this metric is used by the TPS module to eliminate false alarms, and thus is not used by the DR25 Robovetter.

- ModelChiSquareGof-sig: The significance of the  $\chi^2_{(\text{GoF})}$  discriminator as described in Twicken et al. (2016). If this value is close to 100%, then it indicates the model well fits the flux time series data. If this value is close to 0%, then the model fit to the data is poor, and the event is likely a false positive. Note that this metric is used by the TPS module to eliminate false alarms, and thus is not used by the DR25 Robovetter.

- Bootstrap-pfa: The probability of a false alarm (pfa) due to statistical fluctuations, as calculated by Jenkins et al. (2016). The transit detection is considered more credible the closer the value is to zero. In essence the test works by searching the transit-removed data for signals with the same period and duration as the TCE – if signals of comparable strength are found the validity of the original TCE is called into question. Technically speaking, the bootstrap-pfa compares the distribution of MES values that result when searching the transit-removed data at the same period and duration as the original TCE, to the MES of the original TCE (see chapter 10 of Jenkins 2017 for a detailed explanation).

- RollingBand-fgt: The fraction of good transits (fgt) coincident with rolling band image artifacts at durations near the transit duration associated with the TCE. Good transits are those that occur on cadences for which the rolling band severity level = 0, i.e., no rolling bands are detected. The values in brackets are the number of transits at severity level = 0 / the total number of transits on cadences with rolling band diagnostics. Rolling band diagnostics are not available for certain quarters, so their transits are not represented in the denominator.

- GhostDiagnostic-chr: The ratio of the core to halo aperture correlation statistics for the optical ghost diagnostic test (see chapter 11.3.7 of Jenkins 2017). This test calculates the correlation of the TCE signal with two separate light curves — one created using the average of the pixels inside the target's optimal aperture minus the average of the pixels in an annulus surrounding the target aperture (core aperture correlation statistic), and the other using the average of the pixels in the annulus surrounding the target aperture (halo aperture correlation statistic). GhostDiagnostic-chr is displayed in red if the core aperture correlation statistic is less than the

halo aperture correlation statistic, which indicates that the source of the transit signature is not likely to be contained in the optimal aperture associated with the target star.

- Centroid-sig: A measure of whether there is a statistically significant (sig) centroid shift correlated with the transit signature as measured by flux-weighted centroids. A Centroid-sig value near 0% indicates that a flux-weighted centroid shift is detected, however this method is unreliable if there is any significant amount of light from nearby stars in the target's aperture.
- Centroid-so: The measured angular distance between the target star position and the location of the transiting source, determined from the in- and out-of-transit flux-weighted centroid shift. This helps determine if there is a significant offset (so) between the target and the source of the transit signal. The measurement significance is shown in brackets.
- OotOffset-rm: The measured angular distance between the quarterly-averaged out-of-transit source location and the quarterly averaged location of the transiting source, both determined via PRF fitting, utilizing a robust mean (rm). The measurement significance is shown in brackets.
- KicOffset-rm: The measured angular distance between the quarterly-averaged transit location determined via PRF fitting and the target star position listed in the KIC, using a robust mean (rm). The measurement significance is shown in brackets.
- OotOffset-st: The number of quarters for which offsets of the transit source from the out-of-transit (OOT) source location were successfully computed, as determined from PRF fitting. The data is broken down into each season (S1/S2/S3/S4) with the season total (st) number shown in brackets. This is useful to determine if the centroid measurements are all in the same season.
- KicOffset-st: The number of quarters for which offsets of the transit source location from the target star position listed in the KIC were successfully computed, using PRF fitting. The data is broken down into each season (S1/S2/S3/S4) with the season total (st) number shown in brackets. This is useful to determine if the existing centroid measurements are from multiple seasons, or if they are all from the same season, which may indicate a bias.
- DiffImageQuality-fgm: A measure of the quality of the PRF fit to the difference images. The correlation between the fitted PRF and the difference image is computed for each quarter; when the correlation is  $> 0.7$  the fit is declared to be "high-quality". (PRF fits that are not high quality are not necessarily invalid and are used in the centroid offset plot, though examination of the pixel images in the full DV report is recommended to determine their validity.) The reported value is the fraction of quarters with successful PRF fits that were deemed "high-quality", also known as the fraction of good measurements (fgm). The numbers in brackets are the number of quarters with high-quality centroids and the number of quarters with a successful PRF fit.
- DiffImageOverlap-fno: The fraction of difference images that are generated from non-overlapping transits only. Transits that overlap transits associated with other TCEs on the same star are not excluded from computation of a difference image if doing so would leave no clean transits in the given quarter. The two values in brackets are the number of quarters with difference images based on non-overlapping transits / the total number of quarters with difference images. Difference images based on overlapping transits may be very difficult to interpret; caution is advised.

## Pages 2 & 3 – PDC Flux Plots

The photometric data shown in the DV Summary has been processed by the pre-search data conditioner (PDC), the harmonic removal algorithm in TPS, and then either a median filter (Figures 3-5) or the whitener (Figure 6). Occasionally, these steps (in particular the harmonic removal algorithm) can distort astrophysically varying systems in such a way that a variable star appears as a transit-like event. Similarly, systematics may not be completely removed, resulting in low signal-to-noise TCEs that are difficult to identify as due to systematics using the detrended time-series data. Thus, Page 2 contains plots which show the PDC light curve for every quarter, with in-transit cadences highlighted in red against out-of-transit cadences in blue. An example is shown in Figure 11. Page 3 shows the PDC data “stitched” together in the top panel after normalizing each quarter by its median flux value. In the bottom panel the normalized PDC data is shown phase-folded according to the TCE’s period and epoch. Three best-fit sine curves are shown, with their amplitude and phase allowed to vary in the fit, but their periods fixed to the TCE’s period, half the period, and double the period. The sine curves are different colors, with the half, nominal, and double TCE period values shown in the legend for each color. An example is shown in Figure 12.

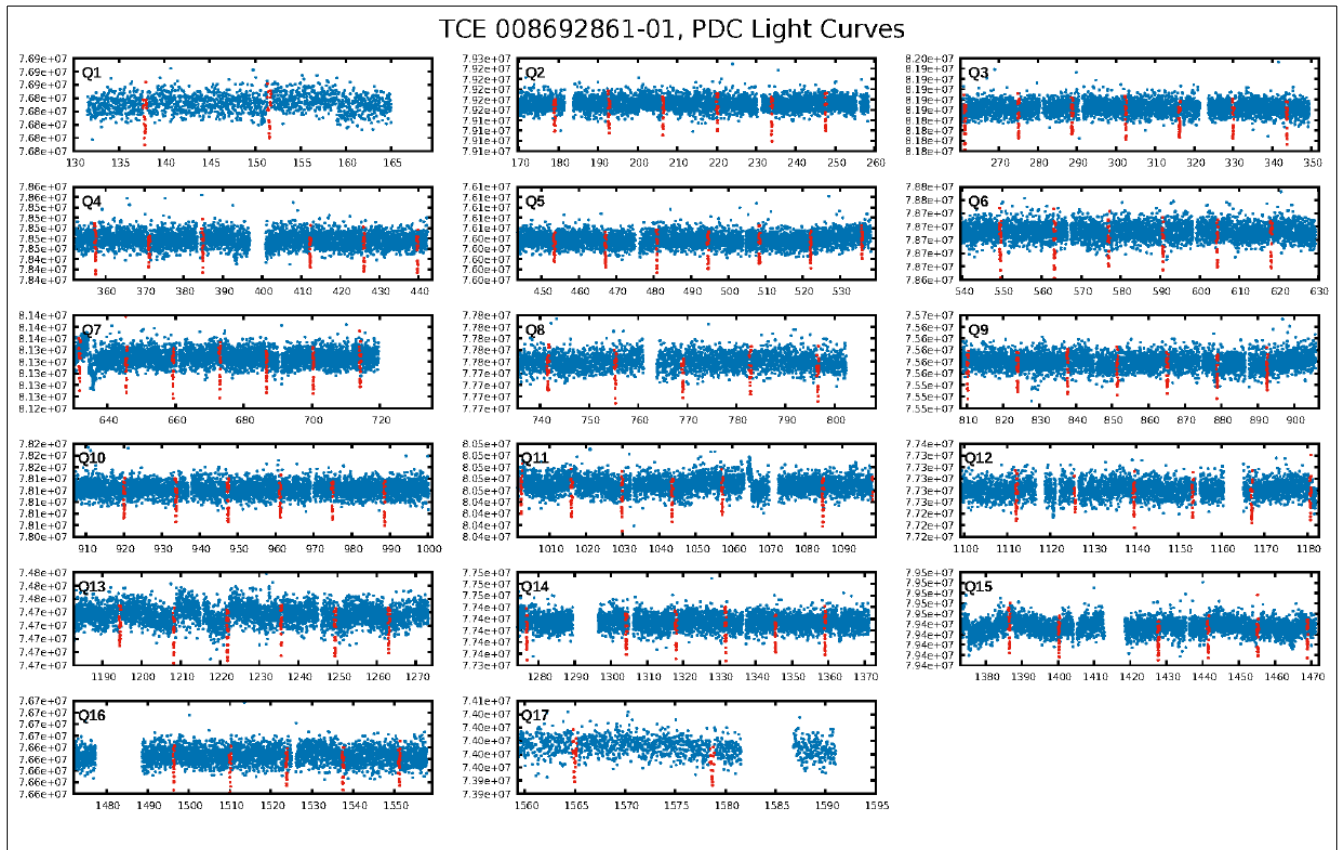


Figure 11: Page 2 of the Kepler Q1–Q17 DR25 TCERT Vetting Reports for each TCE. Each panel contains a different quarter of data, as indicated by each panel’s legend. The PDC data is shown, where red points are in-transit data and blue points are out-of-transit data.

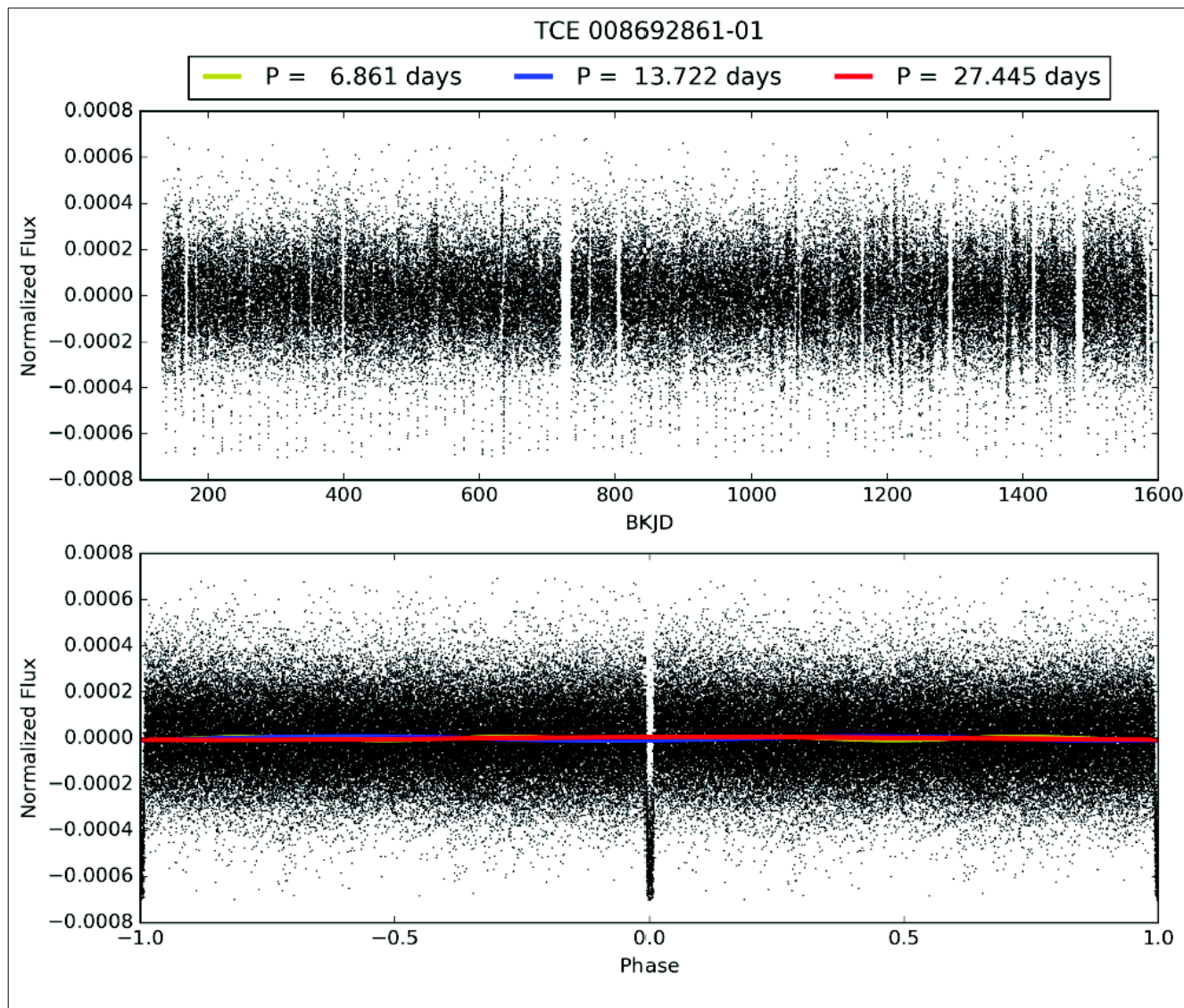


Figure 12: Page 3 of the Kepler Q1–Q17 DR25 TCERT Vetting Reports for each TCE. The top panel shows the PDC time-series flux after each quarter has been normalized using its median flux value. The bottom panel shows the normalized PDC flux phase-folded according to the TCE’s ephemeris. The colored lines represent best-fit sine curves at the TCE’s period, half the period, and double the period. In both panels, extreme outliers are not shown, which may result in transits appearing as truncated.

If the PDC time-series data exhibits strong variability that appears to be not transit-like in nature, and the TCE is detected at a very similar period (or half or double period), it is very likely that the TCE is a FP due to not transit-like variability. In addition, if the locations of the individual transits of a TCE coincide with large systematic features, then it is very likely that the TCE is due to those systematics. Variability or systematics that do not align with the period of the TCE should not be used to designate a TCE as a FP.

### Page 4 & 5 – Odd/Even Plots

As described in the odd/even section of the one-page DV summary, a common source of false positives are eclipsing binaries that have very similar primary and secondary eclipse depths and widths. While a plot of the odd- and even-numbered transits is provided in the DV summary, it is not always easy to distinguish between small depth and/or width variations. Page 4 thus contains a plot of the odd- and even-numbered transits using the DV detrending, overlaid in such a way that small variations are easy to detect by eye. We show an example in Figure 13.

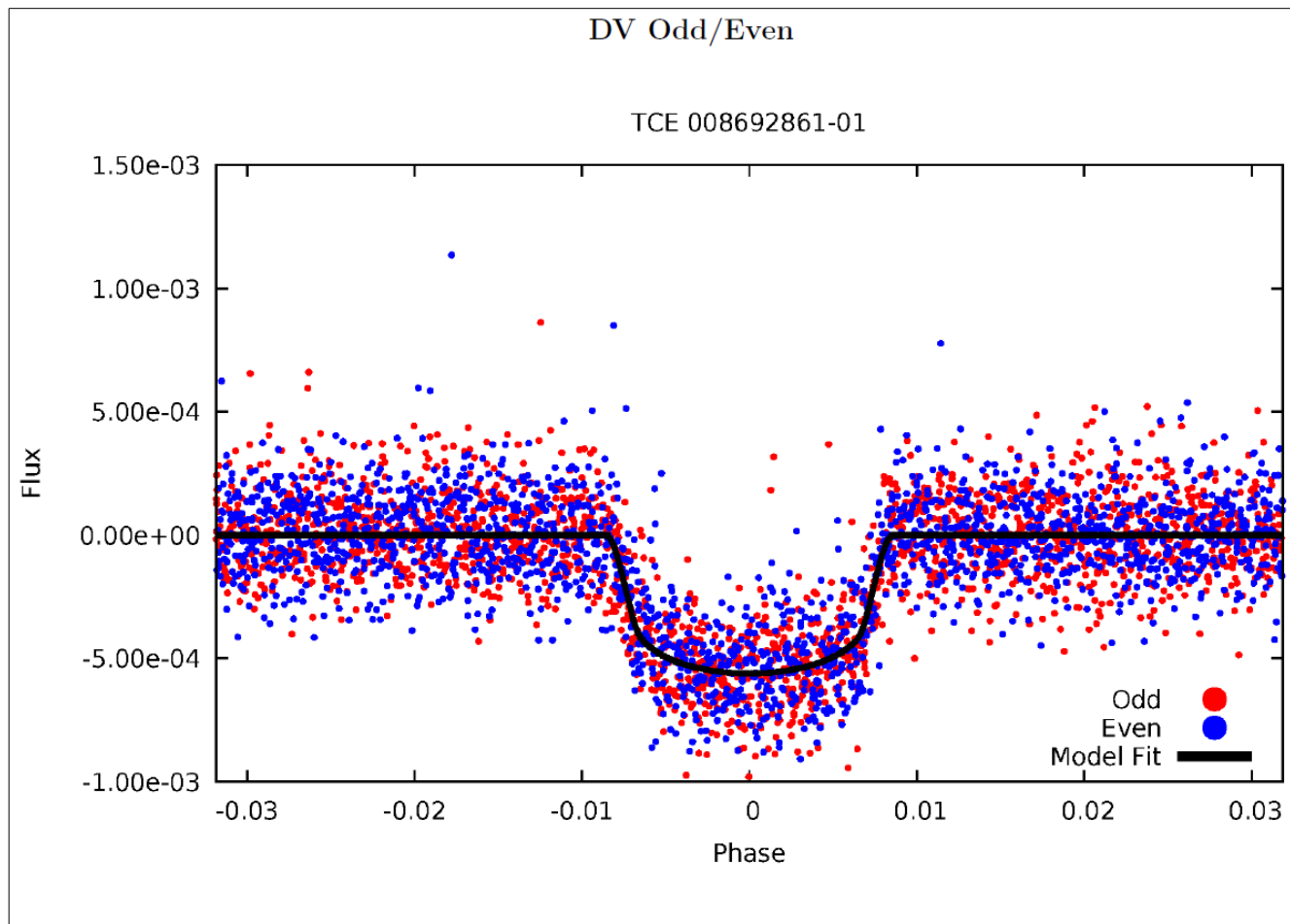


Figure 13: Page 4 of the Kepler Q1–Q17 DR25 TCERT Vetting Reports for each TCE. The DV detrended data is shown phased and zoomed in on the primary transit event. Points from odd- and even-numbered transits are shown by red and blue points respectively. The best-fit transit fit from DV is shown by a solid black line.

TCEs that exhibit coherent, significant differences in the depth, width, or shape of the odd- and even-numbered transits are very likely to be false positives due to an eclipsing binary. One should be careful to verify that any differences are not simply due to systematics or a few outliers. For this reason, TCEs with periods of greater than 90 days (i.e., have one or less transits per quarter) should never be failed as false positives based on an odd/even difference alone.

As discussed above, the DV detrending can sometimes take astrophysically varying systems and greatly distort them in a way that flattens or enhances transit-like events. Thus we employ an alternate (ALT) detrending technique and transit fit for many plots, which specifically is the nonparametric penalized least squares method presented in Garcia (2010), fit by a simple trapezoidal model. Page 5 contains the same odd/even plot as page 4, but utilizes the ALT detrending and trapezoidal model fit. We show an example in Figure 14.

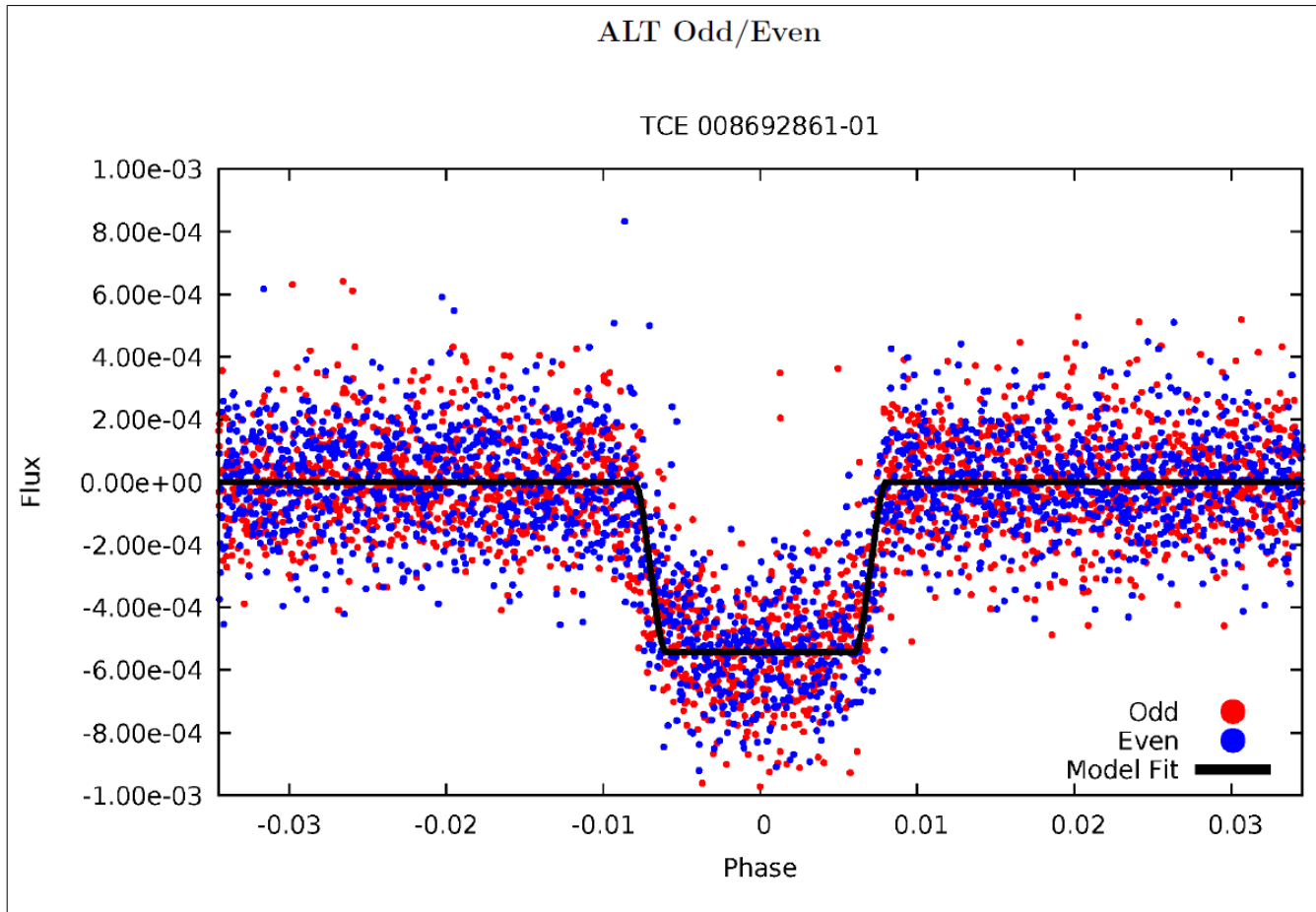


Figure 14: Page 5 of the Kepler Q1–Q17 DR25 TCERT Vetting Reports for each TCE. The figure is identical to Figure 13 / Page 4, but with the ALT detrended data, and the best-fit trapezoidal model fit to the ALT data, shown instead of the DV detrending and DV model fit.

### ***Page 6 – Non-Whitened vs. Whitened Light Curves***

As discussed, detrending algorithms can sometimes affect the data such that not transit-like signals appear as transit-like signals. In the TPS transit search, the final form of detrending is the whiteners, with the search for planetary signals actually occurring in the whitened domain. Page 6 thus shows the phase-folded light curve in both the flux domain (top panel) and the whitened domain (bottom panel). We show an example in Figure 15.

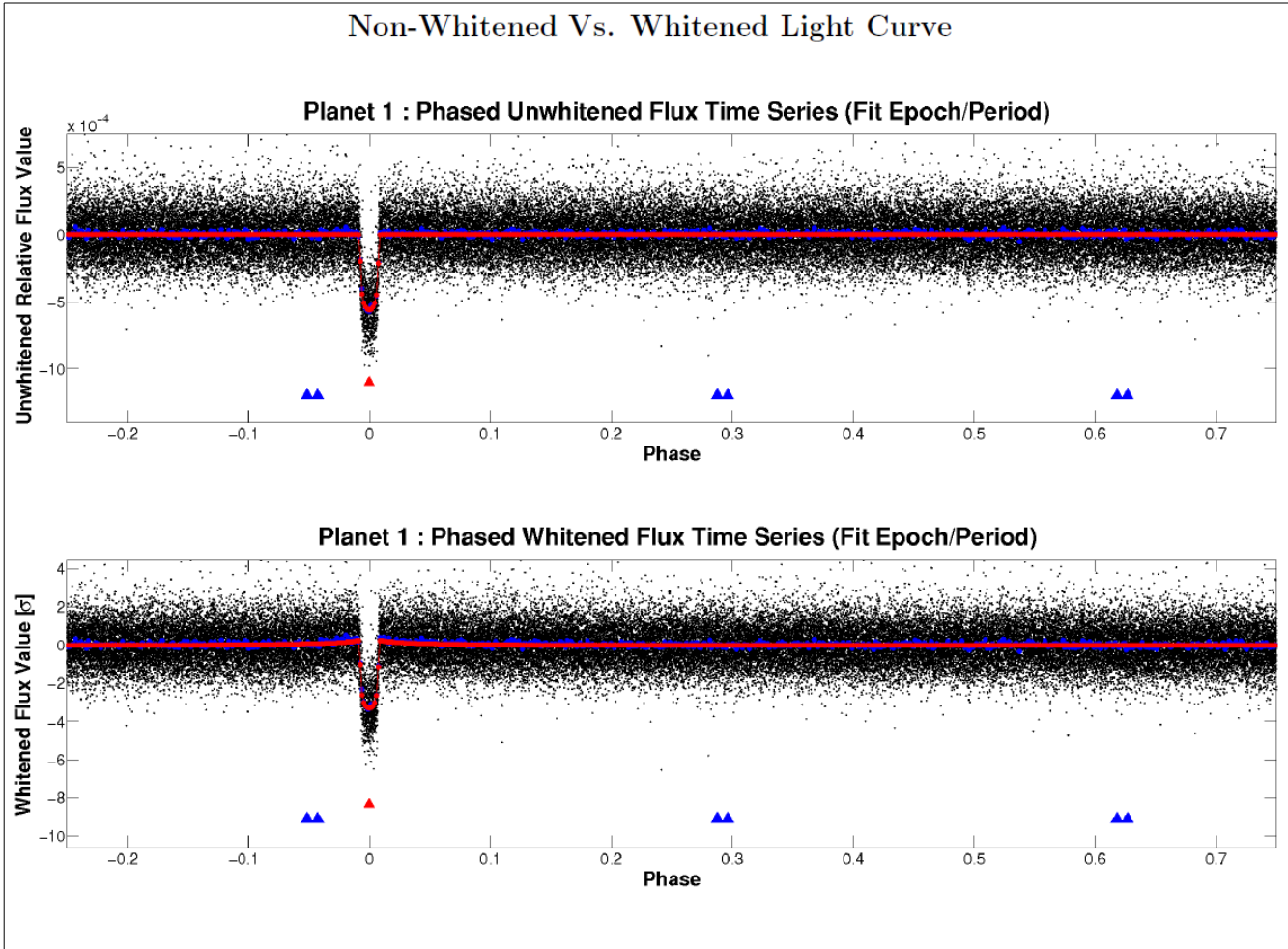


Figure 15: Page 6 of the Kepler Q1–Q17 DR25 TCERT Vetting Reports for each TCE. The top panel shows the phase-folded light curve in the flux domain, while the bottom panel shows the phase-folded light curve in the whitened domain. The transit event is located at phase 0.0 with an upward-facing, red triangle. Upward-facing triangles of other colors show the locations of the primary events of other TCEs in the system, in the phase space of the current TCE under examination.

This page can be used to examine the effect of the whitenner on the data. If strong not-transit-like variability exists on a very similar timescale to the TCE, it can be distorted by the whitenner, so that the signal appears transit-like in the whitened domain. In such cases, the TCE may be a not-transit-like FP that has been made to look transit-like. If variability exists in the unwhitened data on timescales not similar to the transit signal, then the TCE should not be ruled a FP based on this variability alone. In these cases the whitenner is accurately removing variable signals not related to the TCE.

### ***Pages 7, 8, & 9 – Multi-Quarter Transit Plots***

With 17 quarters of data, it is possible to look for quarter-to-quarter and seasonal variations. Extreme variations are often telltale signs of contamination and false-positive identification. As well, when

examining long-period candidates with only a few transits total, it is valuable to look at each individual transit, and in multiple different detrendings, in case any are due to systematics such as sudden pixel sensitivity dropouts (SPSDs), thermal events, spacecraft pointing, etc. (Van Cleve et al., 2016). Zooming in on each individual transit, centered on the time of transit expected from the linear ephemeris, may also reveal transit timing variations.

Pages 7, 8, and 9 show the phased light curve for each quarter, utilizing the PDC, DV, and ALT detrended data, respectively. Each quarter is labeled via Q1 for Quarter 1, Q2 for Quarter 2, etc. To the right of each row of quarters is the combined data for that year, e.g., Year 1 (Y1) is composed of Q1, Q2, Q3, and Q4. At the bottom of each column of quarters is the combined data for that season, e.g., Season 0 (S0) is composed of Q2, Q6, Q10, and Q14. Finally, all data combined for all 17 quarters is shown in the lower-right corner as “All”. Red points are unbinned data and the larger, blue points are binned data. For the DV and ALT data (pages 8 and 9), the best-fit transit model to all the data combined is shown by the solid black line, for all quarters, years, and seasons. We show examples in Figures 16, 17, and 18.

Since the model fit (shown in the DV and ALT detrendings) is constant, it provides a scale for the variation of each individual quarter or yearly/seasonal combination. Thus, if the data for a particular quarter is much deeper than the solid black transit model, it means that the data for that quarter presents a much deeper transit compared to all the data combined. Similarly, if the data appears flat compared to the transit model, then the data for that quarter shows no transit compared to all the data combined. If the period of the system is greater than  $\sim 90$  days, then the transit displayed in each quarter is the only transit observed in that quarter. Finally, small quarter-to-quarter and season-to-season variations are normal, as the star falls on different pixels with different photometric apertures each season.

## ***Pages 10 and 11 – Modelshift Uniqueness Test and Occultation Search***

In the Q1–Q17 DR25 search and analysis, 17 quarters of data were used to search for shallow transit events (less than 100 ppm) with long periods (over 300 days). This means that only a small percentage of the orbital phase contains transit information and it can be very difficult to judge the quality of a detected event when examining either a full phase-curve or a zoom-in on data close to transit. This is simply a fact of the large dynamic range of information that must be assessed to judge a transit candidate. As such, a data product was developed for the Q1-Q12 catalog (Rowe et al. 2015) and employed in all subsequent catalogs, including DR25, to search for additional transit-like events in the data at the same period as the primary event.

If the TCE under investigation is truly a PC, there should not be any other transit-like events in the phase-folded light curve with similar depth and duration as the primary event, in either the positive or negative flux directions. If such signals are present, it calls into question the significance of the primary event. Furthermore, if the primary is unique, and there is a secondary event that is unique and distinct from any other event, it is most likely indicative of an eclipsing stellar binary. Thus, the Modelshift uniqueness test and occultation search can indicate if the TCE under examination is a false alarm due to a source of non transit-like systematics, as well as if it is a false positive due to its signal originating from an eclipsing binary.

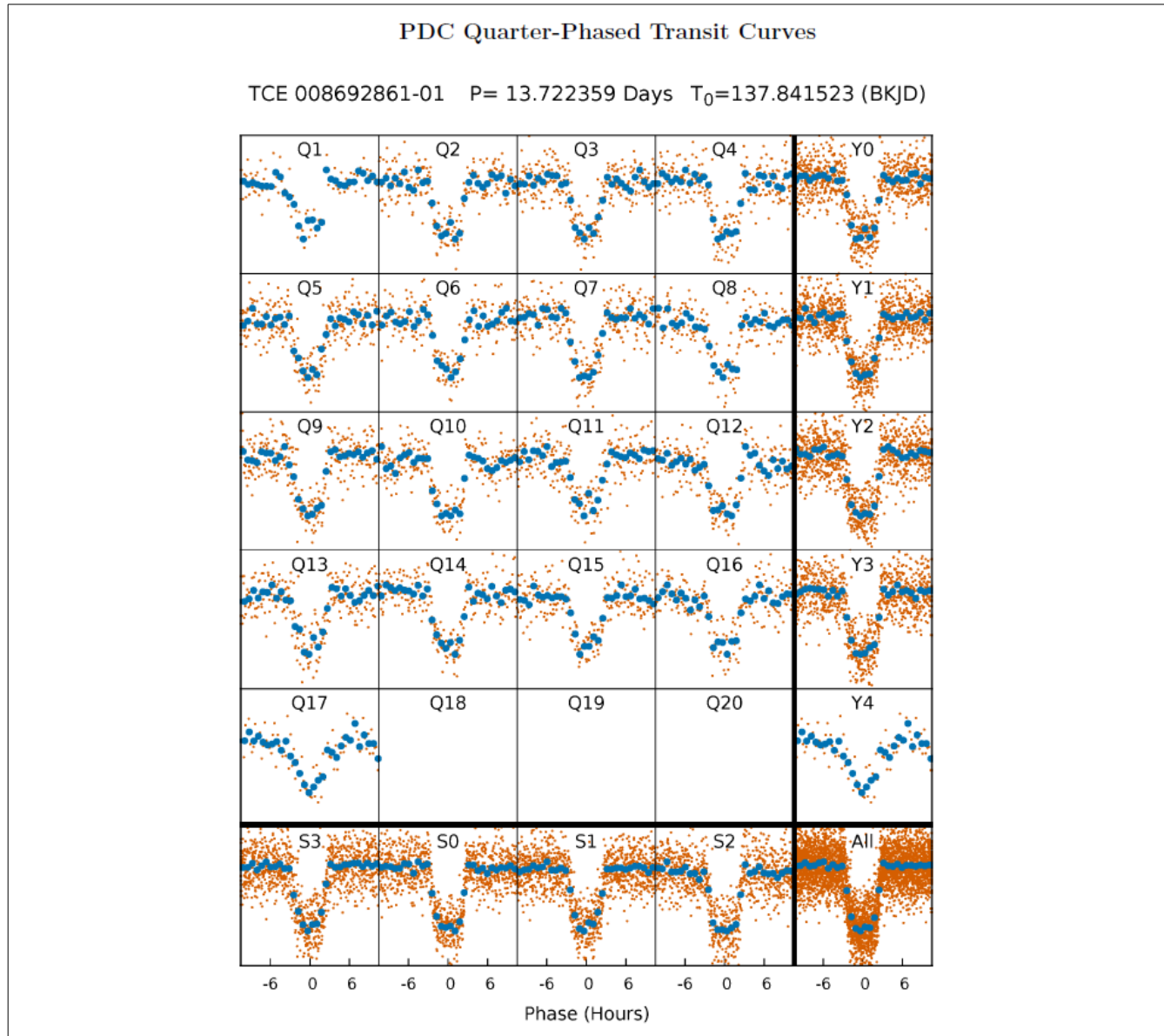


Figure 16: Page 7 of the Kepler Q1–Q17 DR25 TCERT Vetting Reports for each TCE. The top line lists the TCE ID and its associated period and epoch. The boxes show the PDC flux light curve phase-folded to the given period and epoch. Each box is labeled starting with “Q” and followed by the quarter number, up to Quarter 17 (Q17). The boxes labeled starting with “Y” combine all data for the given year, where Year 1 (Y1) contains data from Q1-Q4, Y2 contains data from Q5-Q8, etc. The boxes labeled starting with “S” combine all data for the given season, where Season 0 (S0) contains all data from Q2, Q6, Q10, Q14, S1 contains all data from Q3, Q7, Q11, and Q15, etc. The box in the bottom-right labeled “All” contains all data for the target. Red points represent the raw data and blue points are binned data such that eight binned points will always be located in-transit. Note that no tick marks are shown on the y axis for any box.

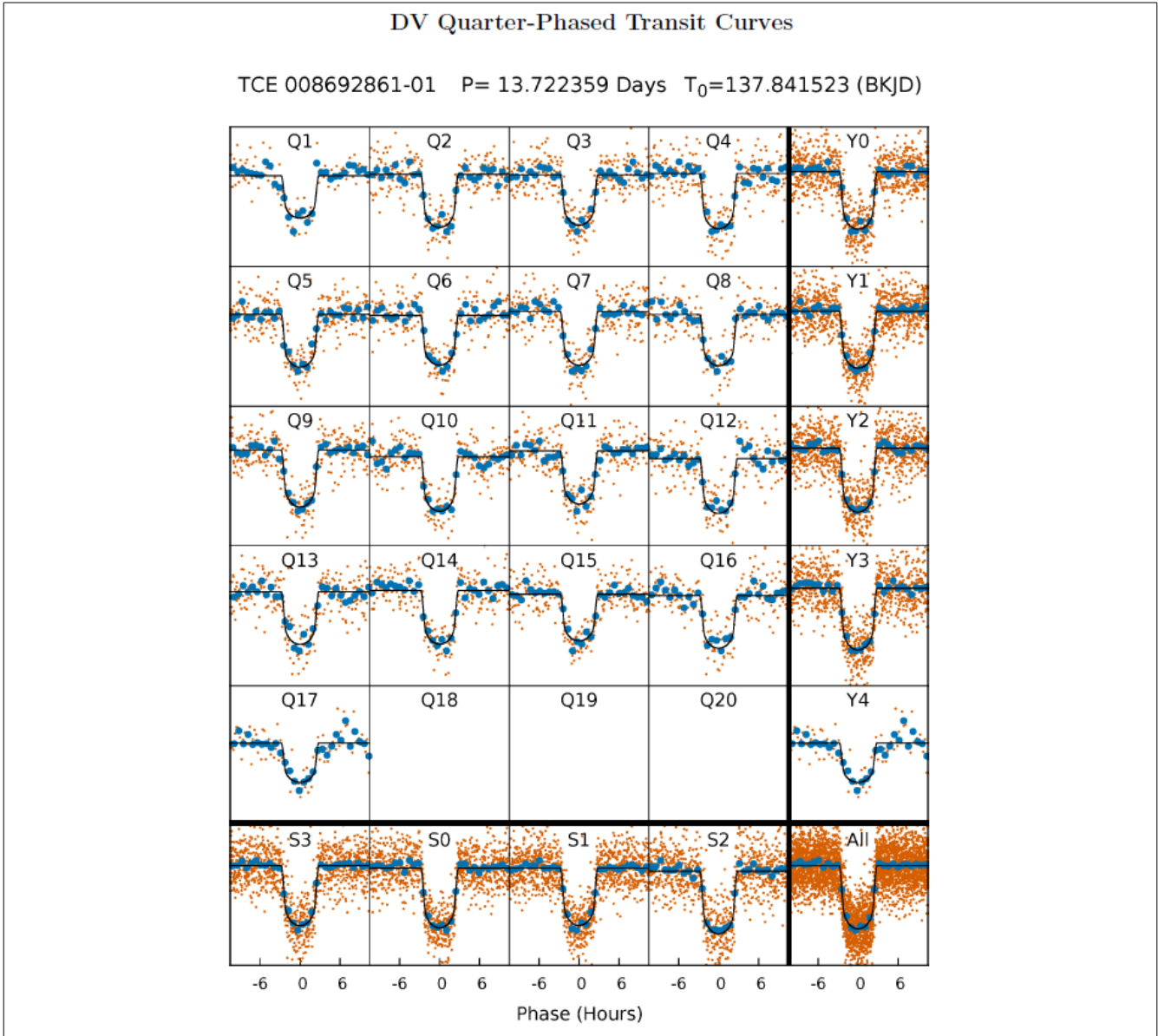


Figure 17: Page 8 of the Kepler Q1–Q17 DR25 TCERT Vetting Reports for each TCE. The top line lists the TCE ID and its associated period and epoch. The boxes show the DV flux light curve phased to the given period and epoch. Each box is labeled starting with “Q” and followed by the quarter number, up to Quarter 17 (Q17). The boxes labeled starting with “Y” combine all data for the given year, where Year 1 (Y1) contains data from Q1-Q4, Y2 contains data from Q5-Q8, etc. The boxes labeled starting with “S” combine all data for the given season, where Season 0 (S0) contains all data from Q2, Q6, Q10, Q14, S1 contains all data from Q3, Q7, Q11, and Q15, etc. The box in the bottom-right labeled “All” contains all data for the target. Red points represent the raw data and blue points are binned data such that eight binned points will always be located in-transit. While no tick marks are shown on the y axis for any box, the DV model-fit (black line) is constant for all boxes and provides a sense of scale.

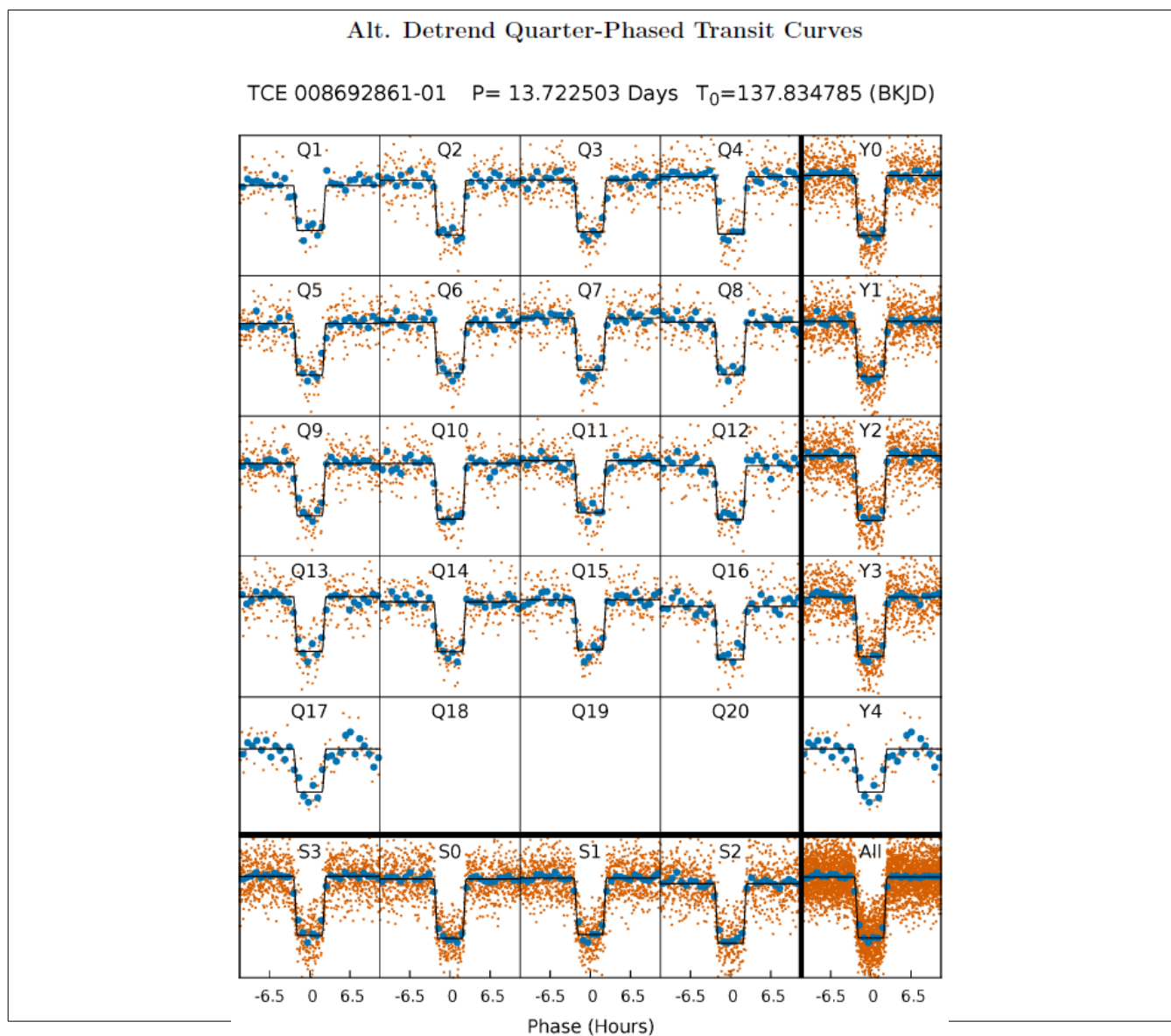


Figure 18: Page 9 of the Kepler Q1–Q17 DR25 TCERT Vetting Reports for each TCE. The top line lists the TCE ID and its associated period and epoch. The boxes show the ALT flux light curve phased to the given period and epoch. Each box is labeled starting with “Q” and followed by the quarter number, up to Quarter 17 (Q17). The boxes labeled starting with “Y” combine all data for the given year, where Year 1 (Y1) contains data from Q1-Q4, Y2 contains data from Q5-Q8, etc. The boxes labeled starting with “S” combine all data for the given season, where Season 0 (S0) contains all data from Q2, Q6, Q10, Q14, S1 contains all data from Q3, Q7, Q11, and Q15, etc. The box in the bottom-right labeled “All” contains all data for the target. Red points represent the raw data and blue points are binned data such that eight binned points will always be located in-transit. While no tick marks are shown on the y axis for any box, the trapezoidal model-fit (black line) is constant for all boxes and provides a sense of scale.

### *Modelshift Uniqueness and Occultation Test Theory*

To search for additional events, we take the DV photometric time series (or ALT) folded at the orbital period of the primary event (e.g., Figure 4) and use the DV-generated transit model (or ALT trapezoidal fit) as a template to measure the amplitudes of other transit-like events at all phases. The amplitudes are measured by fitting the depth of the transit model centered on each of the data points, after rejecting outliers when taking into account the noise at the timescale of the transit duration.

The deepest event aside from the primary transit event, and located at least two transit durations from the primary, is labeled as the secondary event. The next-deepest event located at least two transit durations away from the primary and secondary events is labeled as the tertiary event. Finally, the most positive flux event (i.e., shows a flux brightening) located at least three transit durations from the primary and secondary events is also labeled.

We determine the uncertainty in the amplitude measurements by calculating the standard deviation of the photometric data points outside of the primary and secondary events. Dividing the amplitudes by this standard deviation yields significance values for the primary (Pri), secondary (Sec), tertiary (Ter), and positive (Pos) events. Assuming there are  $P/T_{\text{dur}}$  independent statistical samples per TCE, where  $P$  is the period of the TCE, and  $T_{\text{dur}}$  is the transit duration, we can compute a detection threshold for each TCE such that this test yields no more than one false alarm when applied to all TCEs. We call this threshold  $FA_1$ , and compute it via the following equation,

$$FA_1 = \text{sqrt}(2) * \text{inverfc}[(T_{\text{dur}} / P) * (1 / n\text{TCE})],$$

where *inverfc* is the inverse complementary error function and  $n\text{TCE}$  is the number of TCEs dispositioned. For the Q1–Q17 DR25 activity, for all data types (OBS, INJ, INV, and SCR), we set  $n\text{TCE} = 20,000$ . Similarly, we compute another threshold, called  $FA_2$ , that designates the minimum difference in computed significance between two events in order for the difference to be considered statistically significant,

$$FA_2 = \text{sqrt}(2) * \text{inverfc}[(T_{\text{dur}} / P)].$$

We also measure the amount of systematic red noise in the lightcurve on the timescale of the transit by computing the standard deviation of the measured amplitudes outside of the primary and secondary events. We report the value  $F_{\text{Red}}$ , which is this standard deviation of the measured amplitudes divided by the standard deviation of the photometric data points.  $F_{\text{Red}} = 1$  if there is no red noise in the lightcurve.

In general,  $\text{Pri}/F_{\text{Red}} > \text{FA}_1$  indicates that the primary event is not due to random noise or systematic fluctuations that may occur all throughout the light curve. If  $\text{Pri-Ter} > \text{FA}_2$  and  $\text{Pri-Pos} > \text{FA}_2$  then we believe the transit candidate is unique, i.e., it tells us there is a large difference between the transit event and other putative events in the rest of the phased photometric data, so it is unique even compared to what may be a few systematic events in the light curve. If  $\text{Pri-Ter} < \text{FA}_2$  or  $\text{Pri-Pos} < \text{FA}_2$  then the validity of the transit candidate is called into question because it indicates there are other events in the light curve of comparable depth and signal-to-noise. The presence of an occultation is determined by  $\text{Sec}$  which is a measurement of the significance of the secondary event, analogous to  $\text{Pri}$ . Similar to the primary, a secondary eclipse is generally considered detected if  $\text{Sec}/F_{\text{Red}} > \text{FA}_1$ ,  $\text{Sec-Ter} > \text{FA}_2$ , and  $\text{Sec-Pos} > \text{FA}_2$ , as it is significant compared to systematic noise and unique compared to other events.

In addition to the metrics mentioned above, four new metrics were added to the Modelshift routine in DR25. The first is an Odd/Even test, which is simply the difference in the significance of the primary event as measured by Modelshift separately for the odd- and even-numbered transits. In general, if  $\text{Odd-Even} > \text{FA}_1$ , then there is likely a statistically significant odd/even difference present and the system is likely an eclipsing binary detected at half the true period. The second new test is the Depth Mean-to-Median (DMM) ratio. To compute DMM, Modelshift measures the depth of every individual transit and computes the mean and median of the values. The resulting ratio of the mean to the median is used to identify potential scenarios where the TCE is due to a systematic. If the DMM value is significantly different from 1.0 it indicates that a small fraction of the transits have a significantly different depth from the rest, and thus the TCE is likely systematic in origin and not astrophysical. The third new test is the Shape metric, which measures if the measured amplitudes deviate from the mean value more in the positive flux direction, negative flux direction, or are symmetrically distributed in both directions. Specifically, the Shape metric is defined by

$$\text{Shape} = F_{\text{Max}} / (F_{\text{Max}} - F_{\text{min}}),$$

where  $F_{\text{Max}}$  is the maximum measured flux amplitude and  $F_{\text{Min}}$  is the minimum measured flux amplitude. Note that  $F_{\text{max}}$  is always a positive value and  $F_{\text{min}}$  is always a negative value, as the light curve is normalized, which results in the Shape metric being constrained to a value between 0.0 and 1.0. If this Shape metric is close to 0.0, it indicates the light curve only decreases in flux, as expected for a transiting planet. However if it is near 0.5, it indicates the light curve is either sinusoidal or has both positive and negative flux variations like a heartbeat star. If it is near 1.0 it indicates the TCE's light curve only increases in flux, likely due to a lensing event or a systematic outlier. The fourth new test is the Transit Asymmetry Test (TAT), which is the difference in significance between the left- and right-half of the primary event. If  $\text{TAT}/F_{\text{Red}} > \text{FA}_2$  then there is likely a significant asymmetry present in the shape of the primary event. This typically indicates the event is due to a systematic, though users are urged caution as some planets with significant eccentricity can produce valid, asymmetric transits.

It should be noted that if no DV (or ALT) fit was performed for the given TCE, the Modelshift plots and associated statistics cannot be generated for the given detrending, and do not exist. We show the full Modelshift diagnostic plot page using the DV data and DV model-fit in Figure 19 (page 10), present each individual panel in subsequent plots, and discuss how to use these metrics for vetting. A nearly identical plot using the ALT detrending and trapezoidal model fit is shown on page 11 of the reports.

### Modelshift Metrics

We report 15 measurements at the top of Pages 10 and 11, as shown in Figure 20:

- Pri: The significance of the primary transit. This value will appear in red if  $Pri / F_{Red} < FA_1$ .

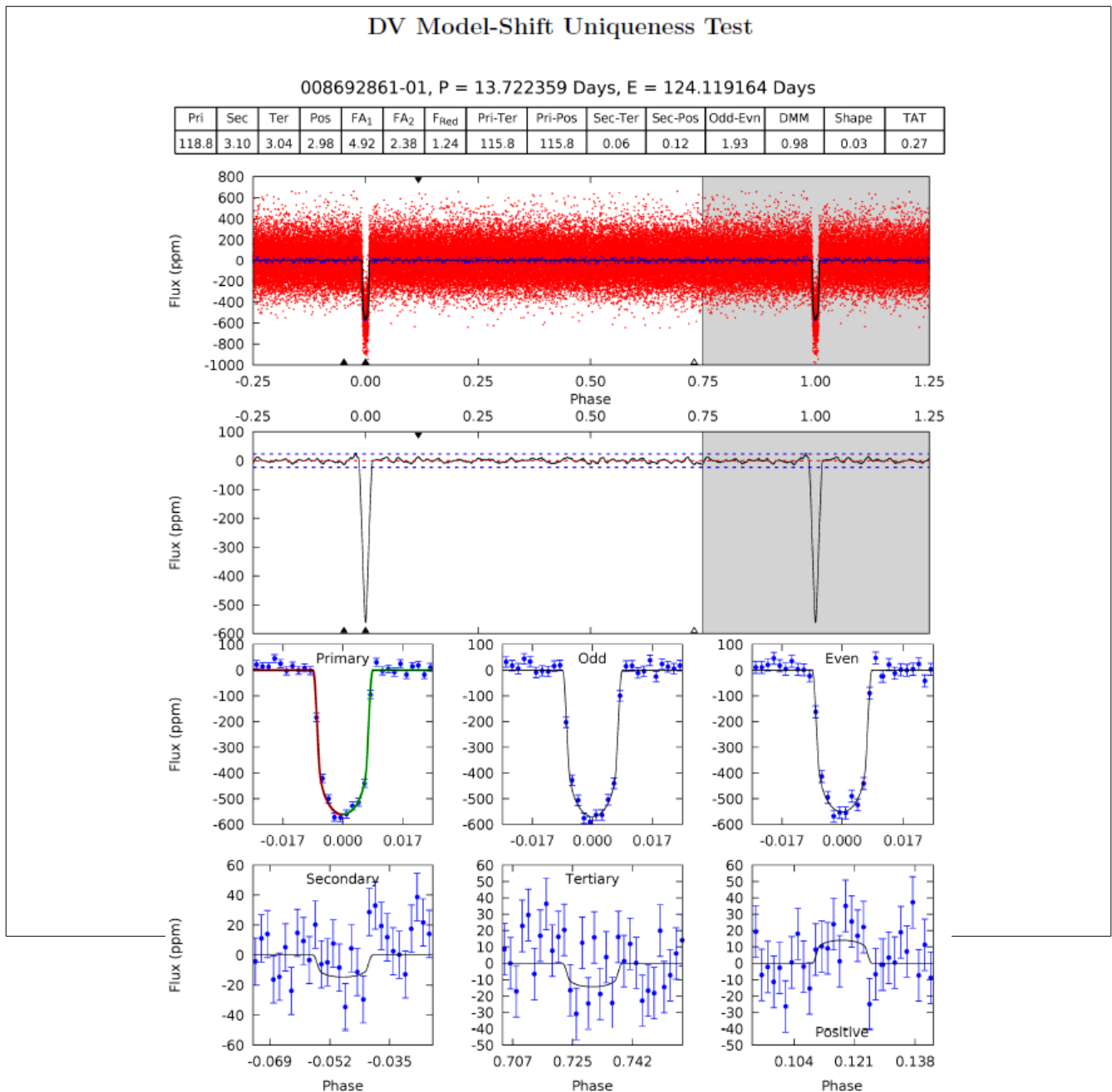




Figure 19: Page 10 of the Kepler Q1–Q17 DR25 TCERT Vetting Reports for each TCE. The top panel shows the values for various metrics computed by the Modelshift test. The second panel (first plot) shows the photometric observations from the DV detrended light curve (see Figure 3) phased to the orbital period of the candidate event. The third panel shows the best-fit depth of the transit model at all phases. The two bottom rows of panels show the primary event in the top left, odd-numbered transits in the top middle, even-numbered transits in the top right, potential secondary event in the bottom left, third strongest transit-like signal (tertiary) in the bottom-middle, and the strongest transit-like signal with increasing flux (positive) in the bottom-right. A nearly identical plot for the ALT detrended data with a trapezoidal transit model fit is shown on page 11 of the reports.

008692861-01, P = 13.722359 Days, E = 124.119164 Days

Pri	Sec	Ter	Pos	FA <sub>1</sub>	FA <sub>2</sub>	F <sub>Red</sub>	Pri-Ter	Pri-Pos	Sec-Ter	Sec-Pos	Odd-Evn	DMM	Shape	TAT
118.8	3.10	3.04	2.98	4.92	2.38	1.24	115.8	115.8	0.06	0.12	1.93	0.98	0.03	0.27

Figure 20: The top line shows the TCE ID and associated orbital period and epoch. The table lists the values for the significances of each event (Pri, Sec, Ter, and Pos), the false alarm detection thresholds (FA<sub>1</sub> and FA<sub>2</sub>), and the ratio of the noise level on the timescale of the transit duration (red noise) divided by the Gaussian noise (F<sub>red</sub>). The difference in significance between the primary and tertiary events (Pri-Ter), the primary and positive events (Pri-Pos), the secondary and tertiary events (Sec-Ter), the secondary and positive events (Sec-Pos), and odd- and even-numbered events (Odd-Evn) are listed next. Finally the values for the DMM, Shape, and TAT tests are shown.

- Sec: The significance of the next deepest event outside of the primary eclipse, which is labeled as a potential secondary. The phase of this event is constrained to be more than two transit durations away from the phase of the primary. This value will appear in red if  $Sec / F_{Red} < FA_1$ .
- Ter: The significance of the third deepest event, aside from the primary and secondary. The phase of this event is constrained to be more than two transit durations away from the phases of the primary and secondary events. This value will appear in red if  $Ter / F_{Red} < FA_1$ .
- Pos: The significance of the strongest positive or 'anti-transit' event. The phase of this event is constrained to be more than three transit durations away from the phases of the primary and secondary events, as the DV detrending can produce positive “shoulders” on the edges of transits/eclipses. This value will appear in red if  $Pos / F_{Red} < FA_1$ .
- FA<sub>1</sub>: The computed detection threshold for each TCE, above which we expect only one detection of a false alarm. Specifically,  $FA_1 = \sqrt{2} \cdot \text{inverfc}[(T_{dur} / P) \cdot (1 / nTCE)]$ , where *inverfc* is the inverse complementary error function, T<sub>dur</sub> is the transit duration, P is the period of the object, and nTCE is the number of TCEs dispositioned. For the Q1–Q17 DR25 TCERT activity we set nTCE = 20,000 for all data type runs. We chose this value as it closely

corresponds to the number of TCEs in the data type with the fewest number of TCEs (INV), and used a constant value for all runs to ensure a consistent fraction of TCEs in each run would fail due to the Modelshift tests that utilize  $FA_1$ .

- $FA_2$ : The computed detection threshold for each TCE when comparing the minimum difference in computed significance between two events in order for them to be considered statistically significantly different. Specifically,  $FA_2 = \sqrt{2} * \text{inverfc}[(T_{\text{dur}} / P)]$ .
- $F_{\text{Red}}$ : The ratio of the level of red noise to the white, Gaussian noise. The level of red noise is computed by taking the standard deviation of the computed amplitudes at all phases outside of the primary and secondary events and dividing by the standard deviation of the photometric light curve outside of the primary and secondary events (see Figure 19).  $F_{\text{Red}} = 1$  if the noise spectrum is white.
- Pri-Ter: The significance difference between the primary and tertiary events. This value will appear red if  $\text{Pri} - \text{Ter} < FA_2$ .
- Pri-Pos: The significance difference between the primary and positive events. This value will appear red if  $\text{Pri} - \text{Pos} < FA_2$ .
- Sec-Ter: The significance difference between the secondary and tertiary events. This value will appear red if  $\text{Sec} - \text{Ter} < FA_2$ .
- Sec-Pos: The significance difference between the secondary and positive events. This value will appear red if  $\text{Sec} - \text{Pos} < FA_2$ .
- Odd-Evn: The significance difference between the odd- and even-numbered transit events. This value will appear red if  $\text{Odd-Evn} > FA_1$ .
- DMM: The ratio of the mean value to the median value of the individual transit depths. This value will appear red if  $\text{DMM} > 1.5$ .
- Shape: The shape metric, which measures if the TCE appears transit-like ( $\sim 0.0$ ), sinusoidal or heartbeat-like ( $\sim 0.5$ ), or lensing-like ( $\sim 1.0$ ). This value will appear red if  $\text{Shape} > 0.3$ .
- TAT: The value of the transit asymmetry test, with higher values indicating an asymmetric transit. This value will appear red if  $\text{TAT} > FA_1$ .

### *Phased Lightcurve*

Similar to Figure 4, Figure 21 shows the *Kepler* DV photometric time-series phased to the orbital period of the primary event. The location of the primary event is marked by an upward, filled triangle at a phase of 0.0. The location of the best secondary eclipse candidate is marked by an upward, filled triangle at a phase other than 0.0. The location of the most significant tertiary event is marked by the location of the upward, open triangle. The location of the most significant positive flux event is marked by the location of the downward, filled triangle.

### Model Filtered Data

Figure 22 shows the measured amplitude of the transit model fitted to each phase-folded photometric measurement. The primary transit is always located at phase zero. A red dashed line is plotted at Flux = 0, with two blue dashed lines marking the fluxes that correspond to  $\pm FA_1$ . This figure is used to evaluate the significance of possible secondary events and, more generally, to help determine the uniqueness of the transit event.

### Primary, Secondary, Tertiary, Positive, Odd, and Even Events

We also present zoomed-in plots of binned photometry for the primary, secondary, tertiary, and positive events, as well as the odd- and even-numbered primary events, as shown in Figure 23. Only the binned data points (in blue) are shown for clarity, with the transit model at the best-fit depth shown via a black line. In the primary plot, the best-fits to the left and right halves of the primary event are shown by red and green lines respectively. These plots can be very useful for establishing the credibility of the primary and secondary events. Comparison between the DV and ALT detrendings is encouraged to reveal if a particular detrending is distorting the data in an undesired fashion.

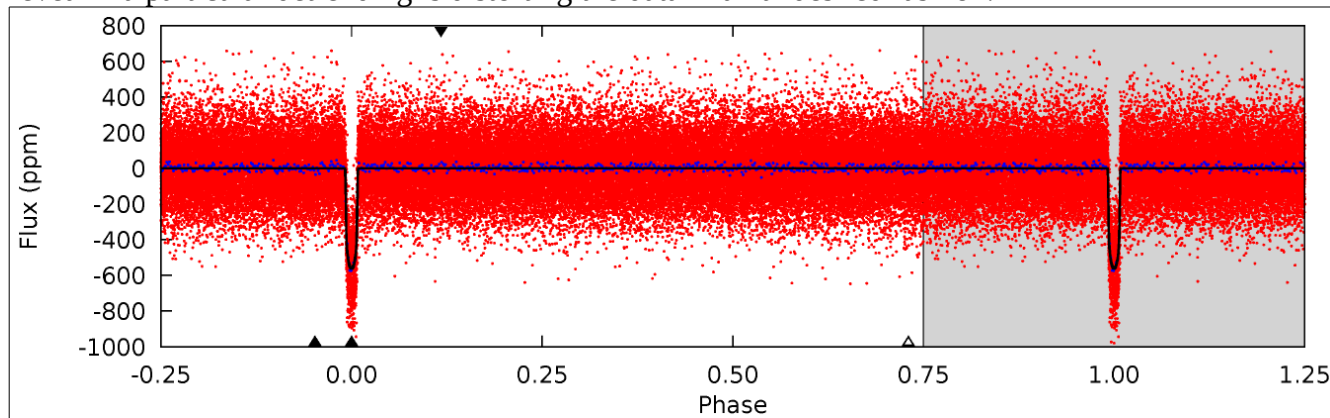


Figure 21: The red points show the phased photometric light curve (in this case the DV detrending) for the candidate event. Blue points show binned data, such that eight binned points lie within the primary transit. In this example, as it is a high SNR planet candidate, the blue points mostly all lie behind the black model line. The black line shows the best-fit transit model (in this case the DV model). The primary event is located at phase zero and is marked by an upward-facing triangle on the bottom axis. The other triangles mark the locations of potential secondary (filled) and tertiary events (open); the location of the strongest *anti-transit* (positive event) is marked by the downward-facing triangle on the top axis. The grayed out area from phase 0.75 to 1.25 plots the same data as is plotted between phases -0.25 and 0.25.

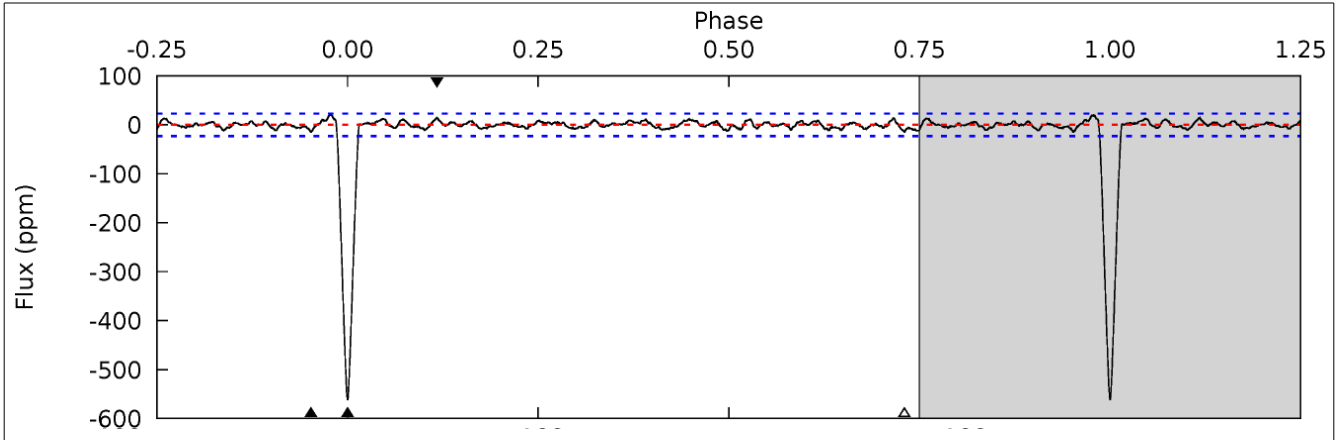


Figure 22: The fitted amplitude of the transit model at each phase-folded, photometric measurement for the given detrending (DV or ALT). A red dashed line is plotted at Flux = 0. The two blue dashed lines mark the fluxes that correspond to  $\pm FA_1$ , which is a Gaussian estimate of a detection threshold that will produce no more than 1 false-alarm for every 20,000 TCEs, assuming white noise. The triangles mark the location of the primary, secondary, tertiary and positive (anti-transit) events as described for Figure 21. Note that in the DV detrending “shoulders” sometimes appear on either side of the primary event as a result of the DV median detrending algorithm.

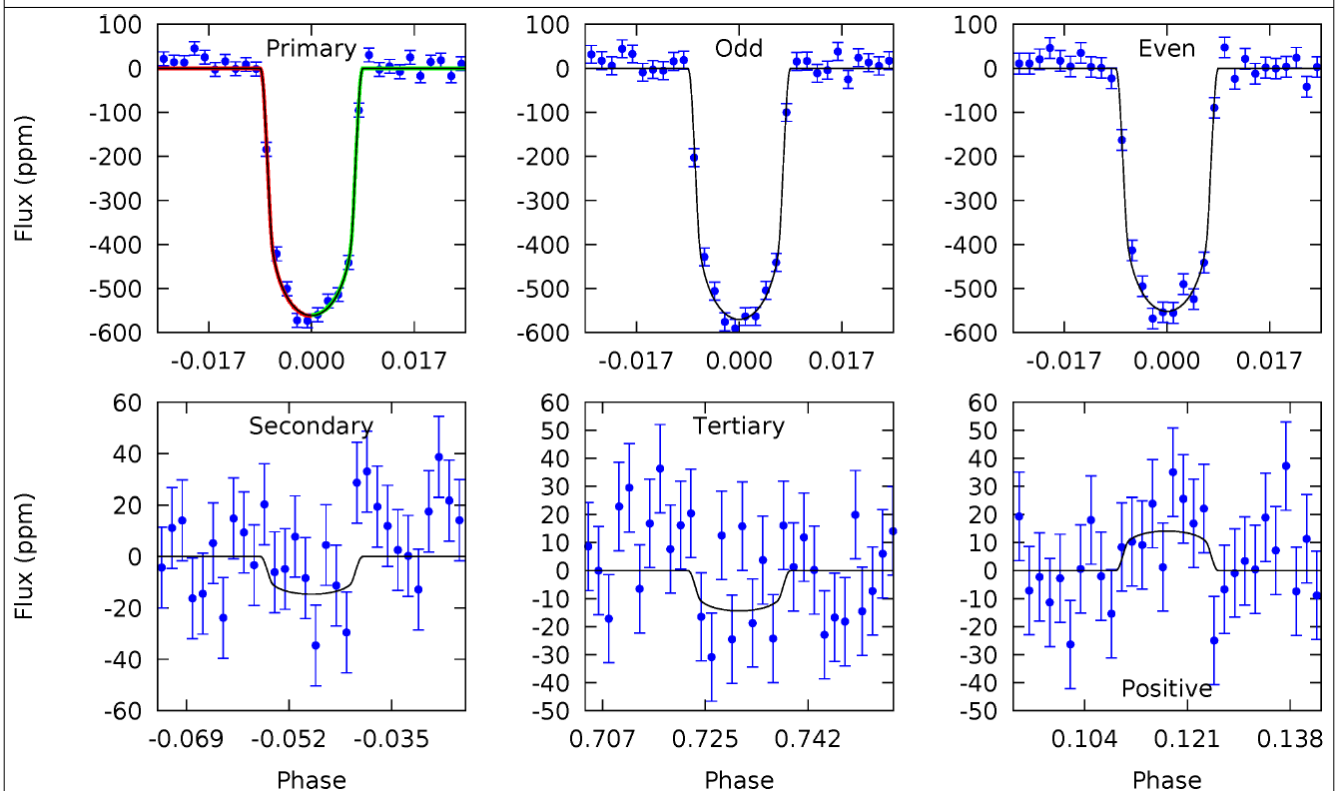


Figure 23: Phased and binned data zoomed in on the primary (top left), odd-numbered (top middle), even-numbered (top right), secondary (bottom left), tertiary (bottom middle), positive (bottom right) events. The solid black line is an overlay of the best-fit transit model to each event.

## ***Page 12 – Stellar Parameters and Secondary Eclipse Tables***

This page provides information on the stellar properties of the star and secondary eclipse parameters of the TCE. An example is shown in Figure 24. The top table shows the values for the effective temperature, surface gravity, metallicity, radius, mass, and density of the host star as determined by Mathur et al. (2017). For each value the asymmetric, one-sigma gaussian error bars are also shown. The next row lists the error bars as a percentage of each parameter's value. The last row lists the provenance of each value, as described in Mathur et al. (2017), and also summarized in the text below the table.

The second table lists the secondary eclipse parameters for the TCE as determined by the Modelshift test applied to both the DV and ALT detrendings. The depth of the secondary eclipse is given along with an error as determined from the gaussian noise of the light curve, where negative flux values indicate a decrease in flux for the secondary, as expected. This depth and corresponding errors are then convolved with the stellar parameters and corresponding errors in a Monte Carlo routine to produce several physical parameters of interest and corresponding errors. (The resulting median and +/- 1 sigma errors from the Monte Carlo routine are reported). The planetary radius ( $R_p$ ) is calculated by multiplying the radius ratio from the DV model fit by the stellar size in the above table.  $T_{max}$  is the maximum possible day-side effective temperature of the planet, assuming no re-radiation of heat from the day side to the night side.  $T_{obs}$  is the calculated day-side effective temperature that would be needed to reproduce the observed secondary eclipse depth, assuming an albedo of 0.3 and that the planet and star radiate as perfect blackbodies. Finally,  $A_{obs}$  is the albedo needed to reproduce the secondary eclipse depth, assuming no thermal emission at visible wavelengths.

Stellar Parameters For KIC 008692861

	$T_{\text{eff}} (K)$	$\log(g)$	$[\text{Fe}/\text{H}]$	$R (R_{\odot})$	$M (M_{\odot})$	$\rho_{\star} (\text{g}\cdot\text{cm}^{-3})$
	$5637^{+113}_{-101}$	$4.399^{+0.132}_{-0.088}$	$-0.300^{+0.150}_{-0.150}$	$0.943^{+0.117}_{-0.117}$	$0.813^{+0.072}_{-0.036}$	$1.365^{+0.774}_{-0.351}$
	+2%/-2%	+3%/-2%	+50%/-50%	+12%/-12%	+9%/-4%	+57%/-26%
Source	SPE48	SPE48	SPE48	DSEP		

KIC = Kepler Input Catalog; PHO = Photometry; SPE = Spectroscopy; AST = Asteroseismology  
 TRA = Transits; DESP = Dartmouth Models; MULT = Multiple Models

Secondary Eclipse Parameters for KIC 008692861-01 / KOI 0172.01

Detrend	Depth (ppm)	$R_p (R_{\oplus})$	$T_{\text{max}} (K)$	$T_{\text{obs}} (K)$	$A_{\text{obs}}$
DV	$-15 \pm 5$	$2.41^{+0.26}_{-0.25}$	$1040^{+43}_{-45}$	$2947^{+145}_{-163}$	$15^{+7}_{-5}$
Alt.	$-17 \pm 5$	$2.39^{+0.26}_{-0.25}$	$1041^{+41}_{-40}$	$3020^{+141}_{-155}$	$18^{+8}_{-6}$

$T_{\text{max}}$  = Theoretical Maximum Planetary Temperature  
 $T_{\text{obs}}$  = Observed Planetary Temperature (Assuming  $A=0.3$ )  
 $A_{\text{obs}}$  = Observed Albedo (Assuming  $T=0$ )

If a secondary eclipse is present, the system is likely an EB if  $T_{\text{obs}} \gg T_{\text{max}}$  AND  $A_{\text{obs}} \gg 1.0$

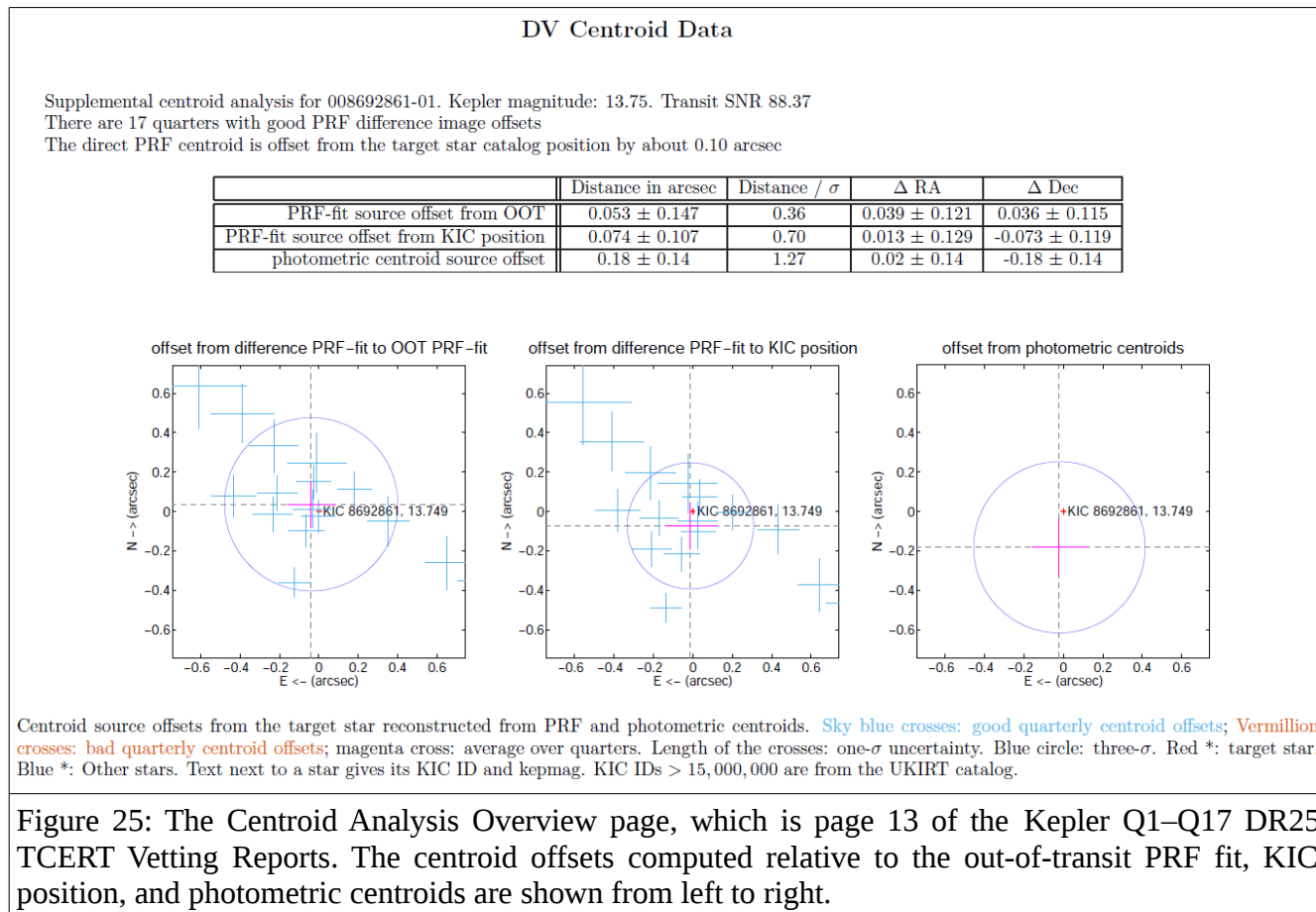
Figure 24: Tables of the stellar and secondary eclipse parameters for the given TCE, which is page 12 of the Kepler Q1–Q17 DR25 TCERT Vetting Reports. If a significant secondary was detected in either the DV or ALT detrending via the Modelshift uniqueness test, then the second table can be used to determine if the secondary eclipse is possibly planetary in origin, or is due to a stellar companion.

The values in the bottom table should only be examined if a significant secondary was detected. If so, then this information can be used to determine if the secondary eclipse could possibly be due to planetary reflection and/or emission, or if it must come from a self-luminous stellar object. If  $T_{\text{obs}}$  is significantly greater than  $T_{\text{max}}$ , and  $A_{\text{obs}}$  is significantly greater than 1.0, then this indicates the secondary eclipse is indeed stellar in origin, and the TCE should be classified as a FP. If not, and the object is planetary in size ( $R_p < 30 R_{\text{earth}}$ ), then the TCE should not be classified as a FP on this basis alone.

**Page 13 – Centroid Analysis Overview**

The centroid analysis pages provide more in-depth centroid information than what was presented in Figure 9 for the DV summary. (A similar figure is in the full DV report.) Three different yet complementary reconstructions of the location of the transit signal relative to the target star are shown

in Figure 25.



This page has three elements:

1. Descriptive information about the target:

- a) Kepler magnitude. This is important to identify saturated targets. When the target star is bright enough that saturation may be an issue this value is turned red.
- b) The transit SNR as measured by the DV transit model fit. This will generally indicate the quality of the difference images, as higher SNR (deeper) events will result in higher SNR difference images.
- c) The number of quarters with good difference images. This refers to the difference image quality metric, which tells you how well the fitted PRF is correlated with the difference image pixel data. A difference image fit is considered good if the correlation is > 0.7 — if smaller this does not mean that the quarter’s difference image is useless, just that it must be examined carefully. When the number of good quarters is three or less this line is turned red.

- d) The distance from the out-of-transit PRF-fit centroid to the target star's catalog position. When this distance is  $> 2$  arcsec this line is turned red.
2. A table giving the reconstructed location of the transit signal relative to the target star using three different but complimentary methods:
    - a) The multi-quarter average offset of the PRF-fit difference image centroid from the PRF-fit out-of-transit (OOT) image (see description associated with Figure 9).
    - b) The multi-quarter average offset of the PRF-fit difference image centroid from the Kepler Input Catalog (KIC) position.
    - c) The offset reconstructed from flux-weighted centroids.

For all of these methods the distance, significance, and RA and Dec components are reported. We consider an offset distance to be statistically significant when it is greater than 3 sigma and greater than  $\sim 0.1''$ .

3. Three panels showing the reconstructed location of the transit signal relative to the target star (located at 0,0), which correspond to the three rows of the table. The first two panels, based on PRF-fitting techniques, show the offset from the out-of-transit fit and the KIC position, respectively. In each of these the crosses represent each individual quarter, with the size of the crosses corresponding to their 1-sigma errors. The circle is the 3-sigma result for all quarters combined. The third panel shows the offset location based on photometric centroids, which provides only a multi-quarter result. As discussed previously, one should look to see if any bright stars are near the target that may influence the PRF fit by comparing the calculated offsets from the out-of-transit PRF fit and the KIC position.

For more information on these metrics and the identification of false positives using the pixel-level data, see Bryson et al. (2013) and Mullally (2017).

## ***Pages 14-18 – Pixel-Level Images***

The next five pages show the average difference and out-of-transit images for each quarter, which provide the data behind the PRF-fit centroids and the resulting multi-quarter average. These images are arranged so that they show four quarters, or a full year, per page. Each image shows three positions via markers: “x” marks the catalog location of the target star, “+” marks the PRF-fit centroid of the OOT image, and “Δ” marks the PRF-fit centroid of the difference image. The color bar is a crucial interpretation tool: when it is almost entirely positive for the difference image, this means that the difference image is reliable. When the color bar indicates negative values one should be more cautious. Large negative values are indicated with large, red “X” symbols, and may indicate that the difference images are unreliable, or that the TCE is due to systematics that do not have a stellar PRF. White asterisks indicate background stars with their Kepler ID and magnitudes. This includes stars from the UKIRT catalog, which have Kepler IDs  $> 15,000,000$ . These UKIRT Kepler IDs are internal project

numbers and do not correspond with UKIRT catalog identifiers, but are listed in Appendix B of Bryson and Morton (2017). A N/E direction indicator is provided to allow matching with the figures on page 13 of the reports (see Figure 25).

An example for Q1 and Q2 is shown in Figure 26. The pixels highlighted by a red “X” in the difference image for Q1 represent pixel value variations that are slight increases in light during the transit, but since this quarter contains less data than others (~30 days in Q1 compared to ~90 days in other quarters) and is prone to detrending errors, they do not invalidate the difference image. When the high value pixels in the difference image are isolated and appear star-like we consider this to be a clear transit signal, such as is seen for Q2. When the location of these difference image pixels correspond with the location of the star’s OOT image, we say that the transit signal’s location is consistent with the target star location. In this TCE, for Q1 and Q2 as shown in Figure 26, the difference images are consistent with the OOT images, and thus the transit signal is believed to originate from the target star. No centroid offset is observed.

### ***Page 18 – Folded Flux and Flux-Weighted Centroid Time Series***

This page shows the flux-weighted photometric centroids, which can be used to determine if there is a centroid shift occurring at the time of transit. (Similar figures are in the full DV report.) Unlike the difference images, this plot is guaranteed to exist for every TCE. In Figure 27, the top panel shows the phase-folded DV photometric time-series. The middle and bottom panels show the computed RA and Dec centroid offsets, respectively, for each photometric data point. A photometric offset can be considered to be observed if there is a change in the centroid time series (second and third panel) that looks like the flux time series (top panel).

The purpose of this figure is to verify that if there is a measured photometric shift from the difference images, it looks like the transit signal, and thus is not due to instrumental systematics. However, any amount of light in the aperture not from the target star will cause a centroid shift to appear in this plot, even when the signal does originate from the target star. Thus, this plot should never be used to centroid fail a TCE by itself.

### ***Page 19 – UKIRT Image***

Page 19 shows a UKIRT image centered on the target with a 1' by 1' scale. The image is oriented such that Right Ascension is along the x-axis and Declination is along the y-axis. This UKIRT image can be useful in looking for sources that are close to the target and possibly unresolved in the *Kepler* pixel-level images. An example is shown in Figure 28.

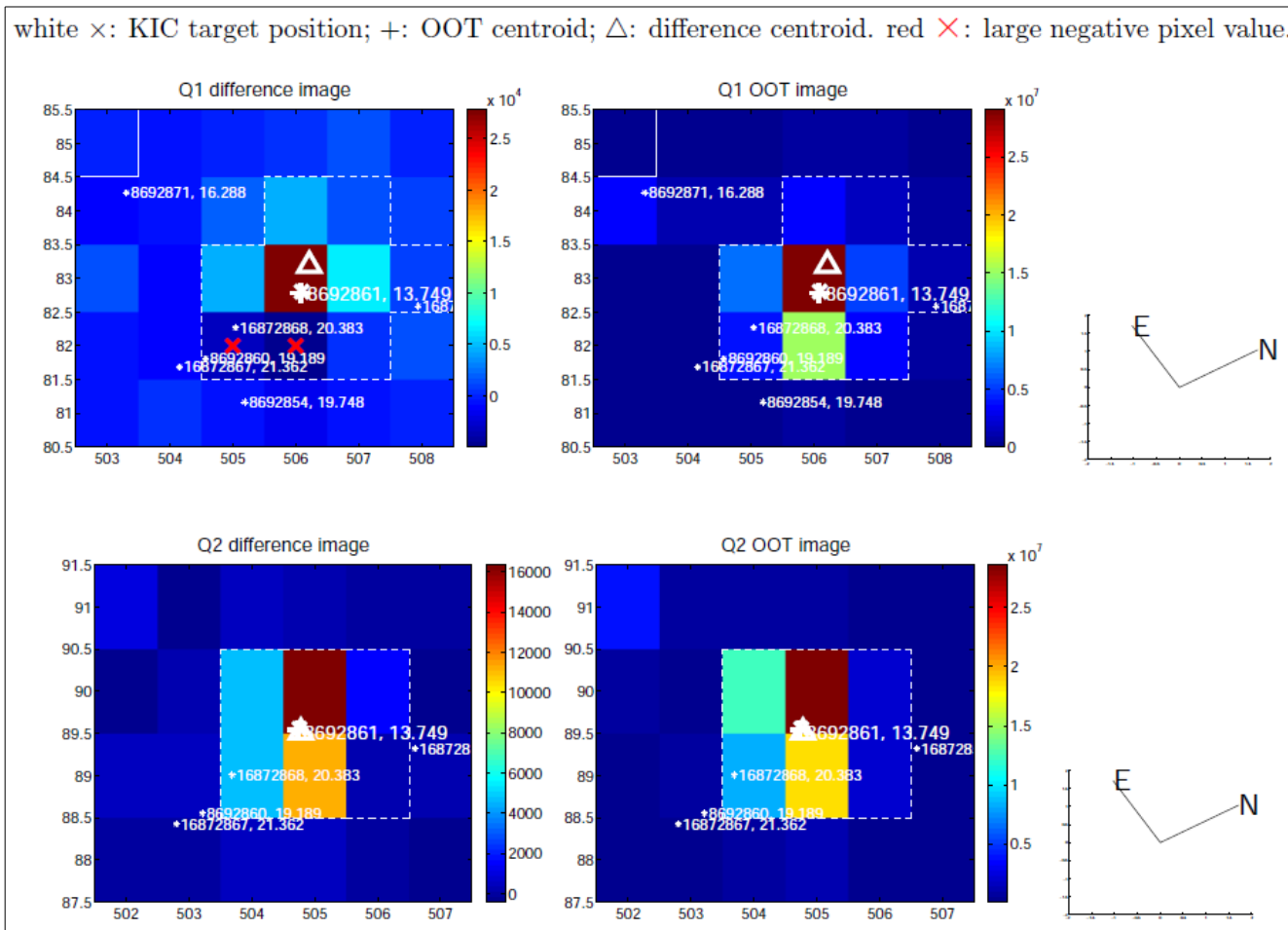


Figure 26: An example of the pixel-level images for Q1 and Q2 for Kepler-69b. The white “x” marks the catalog location of the target star, “+” marks the PRF-fit centroid of the out-of-transit image, and “Δ” marks the PRF-fit centroid of the difference image. Large red “X” symbols indicate negative pixels. In the case of this TCE, the out of transit flux image can be seen to match the difference image very well, indicating the observed transit signal likely originates from the target star.

### Page 20 and Beyond

If there are additional TCEs for the system beyond the first, they will show up as additional pages, replicating those described in Pages 1-19. In each analysis, the in-transit data from previous TCE(s) will have been removed from the data.

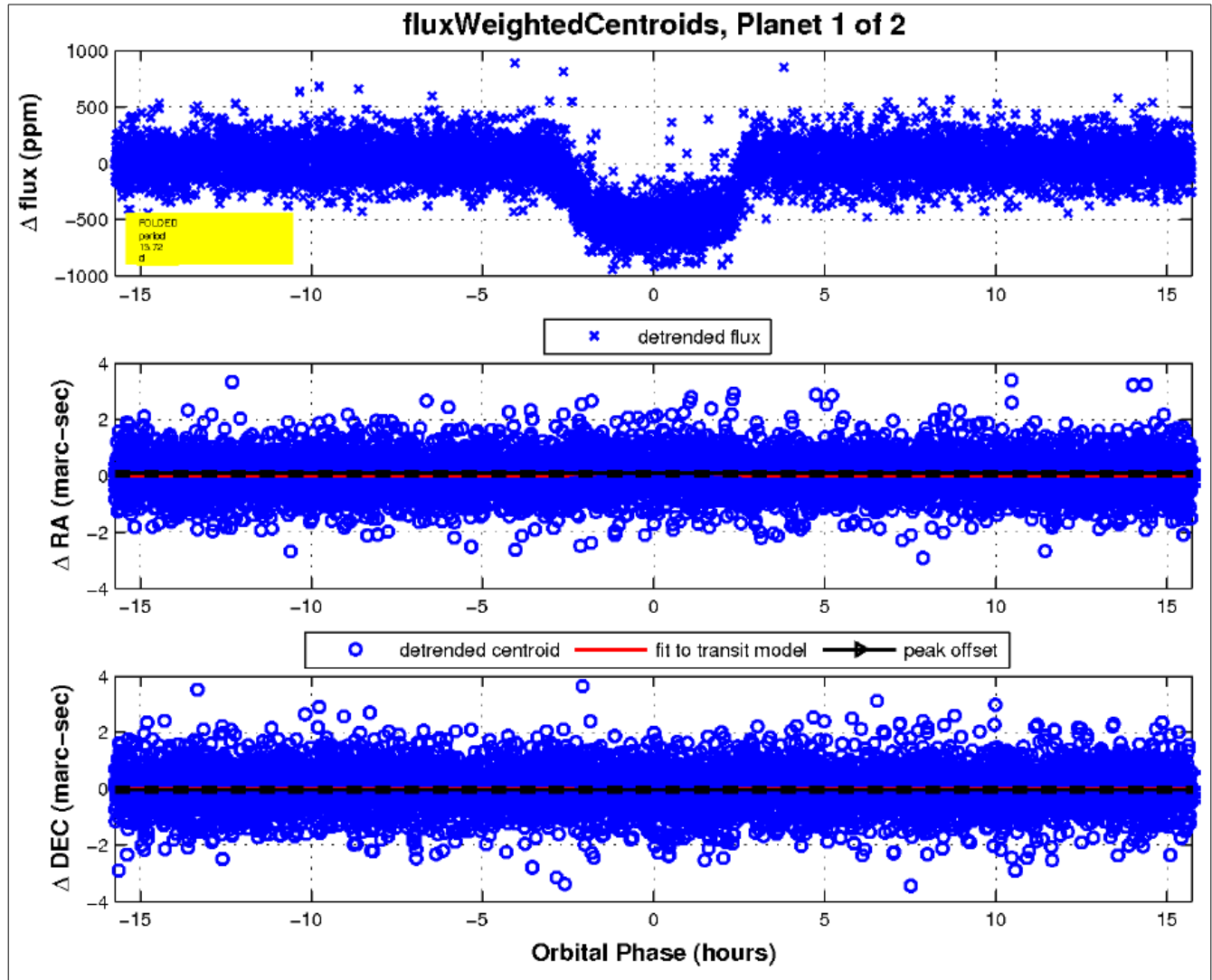


Figure 27: The flux-weighted photometric centroids. Top: The DV phase-folded photometric time series. Middle: The computed RA centroid offset for each photometric data point. Bottom: The computed DEC centroid offset for each photometric data point.

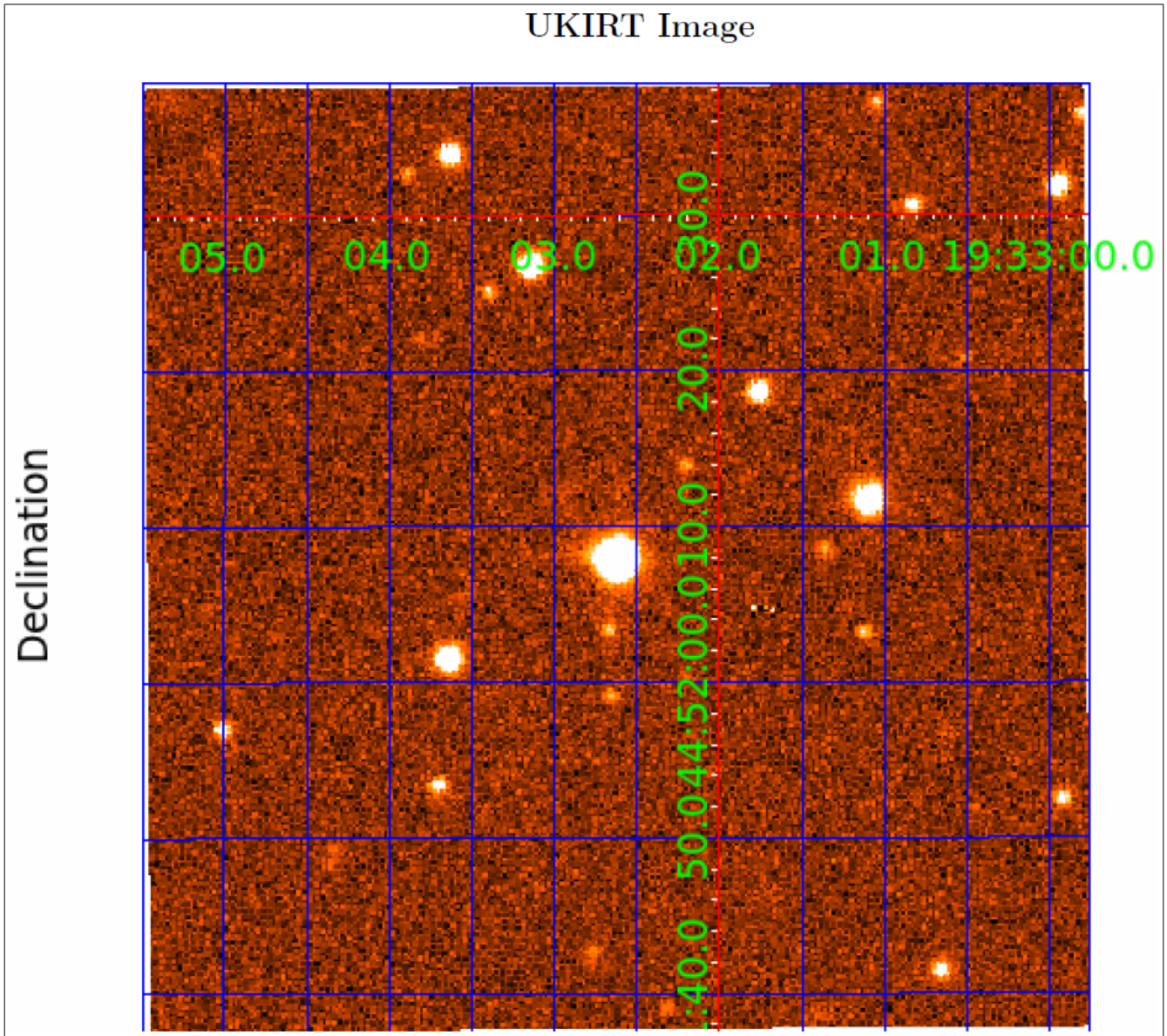


Figure 28: A registered UKIRT image centered on the target with a 1' by 1' scale. The image is oriented such that Right Ascension is along the x-axis and Declination is along the y-axis.

## References

Bryson, S.T., Tenenbaum, P., Jenkins, J.M., et al. 2010, *ApJL*, 713, L97

Bryson, S.T., Jenkins, J.M., Gilliland, R.L., et al. 2013, *PASP*, 125, 889

Bryson, S.T., & Morton, T.D., 2017, Planet Reliability Metrics: Astrophysical Positional Probabilities for Data Release 25 (KSCI-19108-001)

Burke, C. J., & Catanzarite, J. 2017, Planet Detection Metrics: Window and One-Sigma Depth Functions for Data Release 25 (KSCI-19101-002)

Coughlin, J.L., Thompson, S.E., Bryson, S.T., et al. 2014, *AJ*, 147, 119

Coughlin, J.L. 2017, Planet Detection Metrics: Robovetter Completeness and Effectiveness for Data Release 25 (KSCI-19114-001)

Garcia, D. 2010, *Computational Statistics and Data Analysis*, 54, 1167

Jenkins, J.M. and Burke, C.J. 2016, Planet Detection Metrics: Statistical Bootstrap Test (KSCI-19086-004)

Jenkins, J.M. 2017, *Kepler Data Processing Handbook* (KSCI-19081-002)

Mandel, K., & Agol, E. 2002, *ApJL*, 580, L171

Mathur, S., Huber, D., Batalha, N.M., et al. 2017, *ApJS*, 229, 30

Mullally, F. 2017, Planet Detection Metrics: Automatic Detection of Background Objects Using the Centroid Robovetter

Rowe, J. F., Coughlin, J. L., Antoci, V., et al. 2015, *ApJS*, 217, 16

Thompson, S. E., Coughlin, J. L., Mullally, F. M., et al. 2017, *ApJS*, in prep.

Twicken, J. D., Jenkins, J. M., Seader, S. E., et al. 2016, *AJ*, 152, 158

Van Cleve, J., Christiansen, J.L., Jenkins, J.M., et al. 2016, *Kepler Data Characterization Handbook* (KSCI-19040-005)